


RESEARCH ARTICLE



## Bioactivity profiling of *Sanguangporus lonicerinus*: antioxidant, hypoglycaemic, and anticancer potential via *in-vitro* and *in-silico* approaches

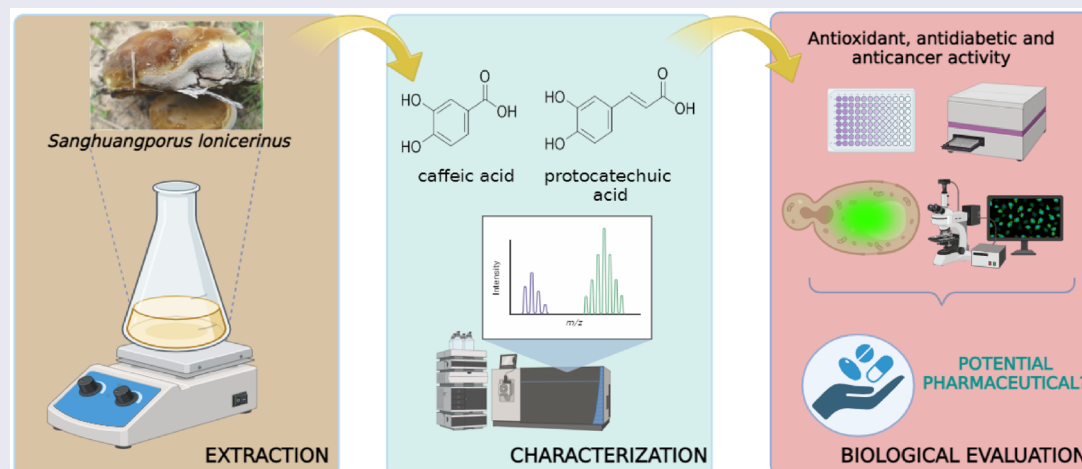
Yusufjon Gafforov<sup>a,b#</sup>, Sofija Bekić<sup>c</sup>, Manzura Yarasheva<sup>d</sup>, Jovana Mišković<sup>e</sup>, Nemanja Živanović<sup>c</sup>, Jia Jia Chen<sup>f</sup>, Edward Petri<sup>g</sup>, Bekhzod Abdullaev<sup>a</sup>, Sylvie Rapior<sup>h,i</sup>, Young Won Lim<sup>j</sup> , Ikram Abdullaev<sup>k</sup>, Arshad Mehmood Abbasi<sup>l</sup>, Soumya Ghosh<sup>m</sup>, Wan Abd Al Qadr Imad Wan-Mohtar<sup>n</sup> and Milena Rašeta<sup>c,e#</sup>

<sup>a</sup>Central Asian Center of Development Studies, New Uzbekistan University, Tashkent, Uzbekistan; <sup>b</sup>Mycology Laboratory, Institute of Botany, Academy of Sciences of Republic of Uzbekistan, Tashkent, Uzbekistan; <sup>c</sup>Department of Chemistry, Biochemistry and Environmental Protection, Faculty of Sciences, University of Novi Sad, Novi Sad, Serbia; <sup>d</sup>Microbiology Laboratory, Navruz International Corp. LLC, Kibray, Uzbekistan; <sup>e</sup>Department of Biology and Ecology, Faculty of Sciences, ProFungi Laboratory, University of Novi Sad, Novi Sad, Serbia; <sup>f</sup>College of Landscape Architecture, Jiangsu Vocational College of Agriculture and Forestry, Zhenjiang, China; <sup>g</sup>Department of Biology and Ecology, Faculty of Sciences, University of Novi Sad, Novi Sad, Serbia; <sup>h</sup>CEFE, Univ Montpellier, CNRS, EPHE, IRD, Natural Substances and Chemical Mediation Team, Montpellier, France; <sup>i</sup>Laboratory of Botany, Phytochemistry and Mycology, Faculty of Pharmacy, Univ Montpellier, Montpellier, France; <sup>j</sup>School of Biological Sciences and Institute of Biodiversity, Seoul National University, Seoul, Republic of Korea; <sup>k</sup>Khorezm Academy of Mamun, Khiva, Uzbekistan; <sup>l</sup>Department of Environmental Sciences, COMSATS University Islamabad, Abbottabad Campus, Abbottabad, Pakistan; <sup>m</sup>Natural and Medical Sciences Research Centre, University of Nizwa, Nizwa, Oman; <sup>n</sup>Functional Omics and Bioprocess Development Laboratory, Institute of Biological Sciences, Faculty of Science, Universiti Malaya, Kuala Lumpur, Malaysia

### ABSTRACT

This study investigates the mycochemical profile and biological activities of hydroethanolic (EtOH), chloroform (CHCl<sub>3</sub>), and hot water (H<sub>2</sub>O) extracts of *Sanguangporus lonicerinus* from Uzbekistan. Antioxidant capacity was assessed using 2,2-diphenyl-1-picrylhydrazyl (DPPH), 2,2'-azino-bis-3-ethylbenzothiazoline-6-sulfonic acid (ABTS), NO, and FRAP assays, and *in vitro* hypoglycaemic effects were evaluated through  $\alpha$ -amylase and  $\alpha$ -glucosidase inhibition. Antiproliferative potential was explored by analysing the binding affinities of EtOH and H<sub>2</sub>O extracts to estrogen receptor  $\alpha$  (ER $\alpha$ ), ER $\beta$ , androgen receptor (AR), and glucocorticoid receptor (GR), with molecular docking providing structural insights. LC-MS/MS analysis revealed solvent-dependent phenolic profiles, with the EtOH extract containing the highest total phenolic content ( $143.15 \pm 6.70$  mg GAE/g d.w.) and the best antioxidant capacity. The EtOH extract showed significant hypoglycaemic effects, with  $85.29 \pm 5.58\%$  inhibition of  $\alpha$ -glucosidase and  $41.21 \pm 0.79\%$  inhibition of  $\alpha$ -amylase. Moderate ER $\beta$  binding suggests potential for estrogen-mediated cancer therapy, while strong AKR1C3 inhibition by the EtOH extract supports its therapeutic potential.

### GRAPHICAL ABSTRACT




### ARTICLE HISTORY

Received 9 October 2024  
Revised 11 January 2025  
Accepted 27 January 2025

### KEYWORDS

Anticancer; diabetes;  
molecular docking;  
phylogeny; polyphenolics

**CONTACT** Yusufjon Gafforov  [yugafforov@yahoo.com](mailto:yugafforov@yahoo.com); [y.gafforov@newuu.uz](mailto:y.gafforov@newuu.uz)  Central Asian Center of Development Studies, New Uzbekistan University, Tashkent, Uzbekistan

 Supplemental data for this article can be accessed online at <https://doi.org/10.1080/14756366.2025.2461185>.

<sup>#</sup>These authors contributed equally to this work.

© 2025 The Author(s). Published by Informa UK Limited, trading as Taylor & Francis Group.

This is an Open Access article distributed under the terms of the Creative Commons Attribution-NonCommercial License (<http://creativecommons.org/licenses/by-nc/4.0/>), which permits unrestricted non-commercial use, distribution, and reproduction in any medium, provided the original work is properly cited. The terms on which this article has been published allow the posting of the Accepted Manuscript in a repository by the author(s) or with their consent.

## Introduction

Mushrooms are a significant source of essential nutrients, including carbohydrates, proteins, vitamins, and minerals<sup>1–3</sup>. Due to their bioactive compounds, certain mushrooms exhibit notable medicinal properties, such as anti-inflammatory, antimicrobial, anti-obesity, antitumor, and antiviral activities<sup>2–10</sup>. Additionally, several medicinal mushrooms have been documented in Uzbekistan, including novel fungi discovered in the study area that are new to science<sup>11–15</sup>. However, these fungi have not been thoroughly scientifically evaluated for their potential in ethnomycology, ethnomedicine and mycochemistry, or as sources of biological actives and bioactive compounds as a member of the Hymenochaetoid taxa<sup>8</sup>.

*Sanghuangporus* species, previously classified as *Phellinus* or *Inonotus*<sup>16,17</sup>, represent one of the most important groups in the family Hymenochaetaceae. They are highly valued for their medicinal properties and have been traditionally used in ethnomedicine across East and Southeast Asia<sup>8,18,19</sup>. In contemporary pharmaceutical research, *Sanghuangporus* spp. have demonstrated a range of beneficial functions. These include enhancing blood circulation, scavenging free radicals, exerting anti-inflammatory effects, combating carcinogenesis, exhibiting antioxidative properties, modulating the immune system, exerting antidiabetic effects, demonstrating antimicrobial activity, and offering anti-aging benefits<sup>20,21</sup>. The genus *Sanghuangporus* was formally established in 2016<sup>22</sup>. To date, over 14 described species of *Sanghuangporus* have been identified globally, with the majority found in Asia<sup>12,23</sup>. The medicinal macrofungus *Sanghuangporus lonicerinus* was first described in 1953 by Soviet mycologist Bondartsev under the name *Phellinus lonicerinus* (Bondartsev) Bondartsev & Singer. It was discovered on *Lonicera* trees in the Samarkand region of Uzbekistan<sup>24</sup>. However, this species has often been confused with the American *Tropicoporus linteus*<sup>25,26</sup>, which has not been found in Eurasia. Similar species restricted to *Lonicera* trees include *S. ligneus* from Iran<sup>27</sup> and *S. lonicericola* from East Asia<sup>22,28</sup>. *S. lonicerinus* is a member of the cosmopolitan family Hymenochaetaceae<sup>8,18,22</sup>. This genus, including *S. lonicerinus*, represents one of the most important groups of medicinal macrofungi and has been utilised in traditional Chinese medicine for over two centuries. In addition, many medicinal macrofungi, including species of *Sanghuangporus*, continue to be of significant interest for their medicinal properties and their traditional uses in ethnomedicine across East and Southeast Asia<sup>19</sup>.

*S. lonicerinus*, also known as the “Reishi of the East”, is a medicinal mushroom that has been used in traditional Chinese medicine for over two centuries<sup>8</sup>. Its widespread use in the Hubei province of China and various other regions, particularly among the Tujia ethnic minority, has been well documented<sup>29</sup>. Recent pharmacological studies have shown that *S. lonicerinus* exhibits diverse biological effects<sup>18</sup>. These include antiproliferative properties, as demonstrated by Wang et al.<sup>30–32</sup>, cytotoxic activity, as reported by Zhang et al.<sup>29</sup>, and both estrogenic and anti-estrogenic effects, as seen by Hu et al.<sup>33</sup>. Additionally, hepatoprotective effects have been observed<sup>34</sup>. However, there is limited scientific literature on *S. lonicerinus*, and its mycochemical composition remains poorly characterised. To date, few compounds have been identified, including polyphenols (hispolon, vanillin, and 3,4-dihydroxybenzalacetone), a fatty acid (docosanoic acid), and sterols (ergosta-6,22-dien-3 $\beta$ ,5 $\beta$ ,8 $\beta$ -triol, ergosterol, and  $\beta$ -sitosterol)<sup>30–32</sup>. Among these, hispolon, a bioactive styrylpyrone polyphenolic compound, has garnered significant attention for its therapeutic potential, particularly in the treatment of cancer and neurodegenerative disorders.<sup>16,18,35</sup>

Despite its historical use and potential, research on *S. lonicerinus* has been slow, hindered by classification problems and a lack

of systematic studies<sup>20</sup>. Oxidative stress, characterised by an imbalance between reactive oxygen species (ROS) production and antioxidant defences, is a major contributor to the pathogenesis of various diseases, such as diabetes and cancer. In diabetes, high glucose levels increase ROS production, causing oxidative damage to pancreatic  $\beta$ -cells and impairing insulin signalling<sup>36</sup>. In cancer, ROS-mediated DNA damage, lipid peroxidation, and protein oxidation drive tumour initiation, progression, and metastasis<sup>37,38</sup>. The potential of natural compounds to combat oxidative stress has garnered significant interest<sup>38</sup>. Extracts of *S. lonicerinus*, rich in phenolic content, exhibit potent antioxidant properties, offering promise as preventive agents against diabetes and cancer. By scavenging ROS and modulating oxidative stress pathways, these extracts may help mitigate disease progression and provide a natural, effective approach to disease management. Hormone-dependent cancers, such as breast and prostate cancer, contribute to a large number of cancer-related deaths globally<sup>39,40</sup>. Since their growth is stimulated by specific steroid hormones, blocking the synthesis and action of these hormones represents a promising treatment strategy. Despite significant advancements in endocrine therapies, there remains a need for the development of more selective and effective modulators targeting steroid receptors and steroid-transforming enzymes. To reduce side effects associated with synthetic anticancer drugs, natural products, such as those derived from mushrooms, are being explored for their potential in cancer treatment<sup>41</sup>. Additionally, mushrooms are increasingly recognised for their importance in this field<sup>30,42</sup>. Based on available literature, hispolon, a polyphenol from *S. lonicerinus*, has demonstrated promising anticancer properties by targeting various signalling pathways; and has exhibited antiproliferative activity against various breast and prostate cancer cell lines<sup>35</sup>.

Through this multifaceted approach, we aim to highlight the significance of conducting mycochemical studies on the neglected macrofungal species of Uzbekistan, showcasing their potential applications in medicinal and therapeutic contexts. Green chemistry (GC) and green analytical chemistry (GAC) have become critical considerations in modern scientific research, ensuring the environmental impact of chemical products and processes is minimised<sup>43</sup>. The concept of GC emerged prominently in the 1990s, with GAC gaining increasing importance in analytical chemistry as standardised tools for evaluating “green profiles” became essential. Notable methods include the Analytical GREENness Metric approach (AGREE), AGREEprep, and the Green Analytical Procedure Index (GAPI), which provide frameworks for assessing the greenness of methodologies. Recent advancements, such as the modified GAPI (MoGAPI), enhance this evaluation, allowing for detailed comparisons between methods using software tools that combine metrics like the analytical Eco-Scale with GAPI<sup>44</sup>. Such tools are vital for ensuring that analytical procedures, such as those used in this study, meet both scientific and environmental standards<sup>43,44</sup>.

In this study, *S. lonicerinus* fruiting bodies were sectioned, air-dried, and stored until extraction. Following established protocols, hot water extracts (H<sub>2</sub>O) were prepared by boiling dried material, filtering, and lyophilising. Hydroethanolic (EtOH) and chloroform (CHCl<sub>3</sub>) extracts were obtained by macerating samples in 70% ethanol (EtOH) or CHCl<sub>3</sub>, followed by filtration and evaporation under reduced pressure. Dried residues were dissolved in dimethyl sulfoxide (DMSO) for storage and further analysis. These methods align with GC principles, balancing environmental impact with analytical efficiency as suggested by Locatelli et al.<sup>43</sup> and Mansour et al.<sup>44</sup>.

In this study, we conducted LC-MS/MS analysis to determine the mycochemical profile of *S. lonicerinus*. The antioxidant capacity

of the extracts was assessed using *in vitro* assays, including anti-2,2-diphenyl-1-picrylhydrazyl (DPPH), 2,2'-azino-bis-3-ethylbenzothiazoline-6-sulfonic acid (ABTS), NO radicals, and FRAP. Additionally, enzyme inhibitory effects were evaluated for their hypoglycaemic potential.

We also investigated the relative binding affinities of EtOH and H<sub>2</sub>O extracts of *S. lonicerinus* for the ligand-binding domains (LBDs) of estrogen receptor  $\alpha$  (ER $\alpha$ ), estrogen receptor  $\beta$  (ER $\beta$ ), androgen receptor (AR), and glucocorticoid receptor (GR) using a fluorescent yeast screen *in vitro*. The potential of *S. lonicerinus* extracts to inhibit specific isoforms of human aldo-keto reductase 1C, which are therapeutic targets for hormone-dependent diseases, was investigated using fluorescence spectroscopy. Lastly, to establish a structural basis for the experimental results and predict the potential binding mechanisms of the quantified polyphenolics with AKR1C3, we performed molecular docking simulations *in silico*.

## Material and methods

### Sample collection and specimen examination

In June 2021, *S. lonicerinus* specimens were collected from mixed broadleaf wild fruit forests in the Western Tien-Shan and northern slopes of the Alay range, Pamir-Alay Mountains, Uzbekistan. The samples were transported to the Mycology Laboratory at the Institute of Botany and stored for further analysis. Macroscopic features were examined using a Leica M165 FC stereomicroscope, while microscopic observations were performed on dried samples with a Leica DM 1000 microscope (up to 1000 $\times$  magnification). The identification of *S. lonicerinus* was confirmed by Yusufjon Gafforov from the Institute of Botany, Uzbekistan Academy of Sciences, and a voucher specimen (TASM6174) was deposited at the Tashkent Mycological Herbarium (TASM), Uzbekistan Academy of Sciences.

### DNA extraction, PCR amplification, and sequencing

Genomic DNA was extracted from fruiting body tissue using the BioSprint 96 DNA Plant Kit (QIAGEN, Germany) with the KingFisher Flex system (Thermo Fisher Scientific, Waltham, MA). PCR amplification targeted the ITS, LSU, and *TEF1* regions, using primers ITS1F/ITS4B, ITS1/ITS4<sup>45,46</sup>, LR/LROR<sup>47</sup>, and EF-983F/EF-1567R<sup>48</sup>. Amplicons were sequenced at the Senckenberg Biodiversity and Climate Research Centre, Goethe University, and the Swedish University of Agricultural Sciences, using the same primers. The assembled sequences were deposited in NCBI GenBank (Supplementary Table 1).

To confirm the identification of the medicinal *S. lonicerinus* from Uzbekistan, sequences for the ITS, LSU, and *TEF1* regions were obtained and combined with additional sequences sourced from GenBank to build a dataset (Supplementary Table 1). *Tropicoporus dependens* (Murrill) L.W. Zhou, Y.C. Dai & Vlasák and *T. guanacastensis* L.W. Zhou, Y.C. Dai & Vlasák, both from the Hymenochaetaceae, were used as outgroup taxa. The ITS, LSU, and *TEF1* regions were aligned using MAFFT version 7, applying the 'G-INS-i' algorithm<sup>49</sup>.

### Phylogenetic study

Phylogenetic analysis was conducted in PAUP\* version 4.0b10<sup>50</sup>, applying the heuristic search method with TBR branch swapping, 1000 random sequence additions, and setting max-trees to 5000. Zero-length branches were collapsed, and all parsimonious trees

were retained. Clade stability was evaluated using 1000 bootstrap replicates<sup>51</sup>. Phylogenetic statistics such as tree length (TL), consistency index (CI), retention index (RI), rescaled consistency index (RC), and homoplasy index (HI) were calculated for each maximum parsimonious tree (MPT) produced, and phylogenetic trees were visualised with Treeview<sup>52</sup>. MrModeltest 2.3<sup>53</sup> was employed to select the most suitable evolutionary model for the Bayesian inference (BI) analysis. BI was executed with MrBayes3.1.2<sup>54</sup> using a general time reversible (GTR) model with a gamma distribution and invariable sites. Four Markov chains were run for 2 million generations, with sampling every 100<sup>th</sup> generation until the split frequency value was <0.01. The first 25% of the trees were discarded as burn-in, and a majority-rule consensus tree was constructed. Treeview<sup>52</sup> was used to visualise the phylogenetic trees, and branch support for maximum likelihood (BS), maximum parsimony (MP), and Bayesian posterior probabilities (BPP) was indicated for values of  $\geq 75\%$  (MP) and 0.95 (BPP).

### Preparation of the extracts for mycochemical study and tested biological activities

Fruiting bodies of *S. lonicerinus* were first divided into sections, air-dried, and stored in opaque containers at room temperature until further processing. All three extracts were prepared following the procedure outlined by Karaman et al.<sup>55</sup> and Rašeta et al.<sup>56</sup>.

**Hot water extracts (H<sub>2</sub>O)** were prepared by boiling dried mushroom parts in water (1:10) and incubating at 80°C for 1 h. After filtration and cooling, the extracts were stored at -20°C, lyophilised for 24 h, and further dried in an ice condenser at -70°C.

**Hydroethanolic (EtOH) and chloroform (CHCl<sub>3</sub>) extracts** were obtained by maceration of mushroom material in 70% ethanol or CHCl<sub>3</sub> (1:10) for 72 h at room temperature. The mixtures were then filtered and evaporated under reduced pressure at 40°C until dry.

Dried residues were dissolved in DMSO and stored at +4°C for further analysis.

### Mycochemical characterisation

#### LC-MS/MS analysis of phenolic compounds

Quinic acid and 44 phenolic compounds (14 phenolic acids, 25 flavonoids, three coumarins, and two lignans) were analysed using LC-MS/MS, based on a previously established method<sup>57</sup>. The analysis was performed using an Agilent 1200 Series HPLC coupled with a 6410A Triple Quad MS, controlled by MassHunter software. Standards were sourced from Sigma-Aldrich, Fluka Chemie, and ChromaDex, and both samples and standards were prepared in 50% methanol (25 mg/mL). A 5  $\mu$ L injection was used, with separation on a Zorbax Eclipse XDB-C18 column. Data were collected in dynamic MRM mode, and peak areas quantified using MassHunter. Calibration curves were created using OriginPro software. Detailed retention times and MS parameters are available in Supplementary Table 2.

#### Quantification of total phenolic, flavonoid, protein, and carbohydrate contents

The total phenolic content (TP) was measured using the Folin-Ciocalteu (FC) method as per Singleton et al.<sup>58</sup>, using an absorbance wavelength of 760 nm. Results were expressed as mg of gallic acid equivalents per gram of dry weight (mg GAE/g d.w.), based on a standard curve.

The total flavonoid content (TF) was determined using an AlCl<sub>3</sub> complexation method, with absorbance at 415 nm and quercetin



as the standard. TF values were reported as mg quercetin equivalents per gram of dry weight (mg QE/g d.w.).<sup>59</sup>

The Lowry method<sup>60</sup> was used to assess total protein content (TPR), based on the reaction of  $\text{Cu}^{2+}$  with Folin reagent. Absorbance was recorded at 740 nm, and TPR was calculated using a BSA standard curve, expressed as mg BSA equivalents per gram of dry weight (mg BSAE/g d.w.).

Total carbohydrate content (TC) was evaluated using the phenol-sulphuric acid method, following Rašeta et al.<sup>56</sup>, with absorbance measured at 490 nm. A glucose calibration curve was used to express TC as mg glucose equivalents per gram of dry weight (mg GluE/g d.w.).

## Examination of biological activities

### Antioxidant activity

Antioxidant activity was evaluated using ABTS<sup>61</sup>, DPPH<sup>62</sup>, NO radical scavenging<sup>63</sup>, and FRAP assays<sup>64</sup>. In the ABTS assay, 290  $\mu\text{L}$  of ABTS reagent (7 mM ABTS and 2.45 mM  $\text{K}_2\text{S}_2\text{O}_8$ ) was added to 10  $\mu\text{L}$  of extract or standard, incubated for 5 min, and absorbance was recorded at 734 nm<sup>61</sup>. For DPPH, 60  $\mu\text{L}$  of 90  $\mu\text{M}$  DPPH solution, 180  $\mu\text{L}$  MeOH, and 10  $\mu\text{L}$  extract/standard were mixed, incubated for 30 min in the dark, and absorbance was measured at 515 nm<sup>62</sup>. NO scavenging was monitored by mixing 15  $\mu\text{L}$  of extract/standard with 250  $\mu\text{L}$  of sodium nitroprusside and phosphate buffer. Following a 90-min incubation period, 500  $\mu\text{L}$  of Griess reagent was added and absorbance was measured at 546 nm<sup>63</sup>. The FRAP assay involved mixing 10  $\mu\text{L}$  of extract/standard with 225  $\mu\text{L}$  FRAP reagent and 22.5  $\mu\text{L}$  distilled water ( $\text{dH}_2\text{O}$ ), followed by measurement of absorbance at 593 nm after 6 min incubation<sup>64</sup>. Results were expressed as mg Trolox equivalents per gram of dry weight (mg TE/g d.w.) for ABTS, DPPH, and NO assays, and as mg ascorbic acid equivalents per gram of dry weight (mg AAE/g d.w.) for FRAP.

### Hypoglycaemic effect

The *in vitro* hypoglycaemic effect was evaluated by assessing the extracts' ability to inhibit  $\alpha$ -amylase and  $\alpha$ -glucosidase, obtained from Sigma-Aldrich (Steinheim, Germany).

Inhibition of  $\alpha$ -amylase was determined using the procedure of Yang et al.<sup>65</sup>, where 90  $\mu\text{L}$  of  $\alpha$ -amylase (porcine pancreas Type VI-B, glucose) was mixed with 80  $\mu\text{L}$  of 0.05% starch in 20 mM phosphate buffer (pH 6.9) and 10  $\mu\text{L}$  of extract or acarbose as standard. After incubating for 10 min at 37°C, the reaction was stopped with 100  $\mu\text{L}$  of cold 1 M HCl and 20  $\mu\text{L}$  of Lugol solution, and absorbance was measured at 620 nm. Results were expressed as % of enzyme inhibition.

For evaluation of  $\alpha$ -glucosidase inhibition, the method from Palanisamy et al.<sup>66</sup> was used, where 100  $\mu\text{L}$  of 0.1 M phosphate buffer (pH 6.8) was combined with 10  $\mu\text{L}$  of  $\alpha$ -glucosidase (*Saccharomyces cerevisiae* Type I), 20  $\mu\text{L}$  of extract or acarbose as standard, and 20  $\mu\text{L}$  of *p*-nitrophenyl  $\alpha$ -D-glucoside. The mixture was incubated for 15 min at 37°C, then 80  $\mu\text{L}$  of 0.2 M  $\text{Na}_2\text{CO}_3$  was added, and absorbance was measured at 400 nm. Results were reported as % of enzyme inhibition.

### Anticancer activity

**Chemicals.** Tryptone, yeast extract, and agar were purchased from Torlak Institute. Synthetic drop-out medium supplement without tryptophan, yeast nitrogen base without amino acids and ammonium sulphate, galactose, kanamycin sulphate, lysozyme Tris,

components for phosphate buffer and 9,10-phenanthrenequinone (PQ) were from Sigma. Bio-Gel P-10 was from Bio-Rad and HisTrap HP columns were from Cytiva. Imidazole, NADPH and sodium chloride were supplied by Carl Roth. DMSO was purchased from Lach-Ner and IPTG from Fisher Scientific. Stock solutions of both extracts were prepared in DMSO and stored at 4°C.

### Fluorescent screen in yeast

Relative binding affinities of EtOH and  $\text{H}_2\text{O}$  extracts of *S. lonicerinus* for LBDs of ER $\alpha$ , ER $\beta$ , AR, and GR were evaluated using a yeast-based fluorescent assay according to our previously described procedure with some modifications<sup>67–70</sup>. *S. cerevisiae* FY250 strain (MAT $\alpha$ , *ura3-52*, *his3 $\Delta$ 200*, *leu2 $\Delta$ 1*, and *trp1 $\Delta$ 63*) was transformed with either pRF4–6-ER $\alpha$  LBD-EYFP, pRF4–6-ER $\beta$  LBD-EYFP, pRF4–6-AR LBD-EYFP, or pRF4–6-GR LBD-EYFP<sup>71</sup>, using a lithium acetate method<sup>72</sup>. Recombinant yeast cells were preincubated with shaking in a Biosan orbital shaker-incubator ES-20/60 for 40 h at 28°C in a tryptophan-selective liquid medium containing 2% raffinose. Cells were then diluted in the same medium to an  $\text{OD}_{600\text{nm}}$  0.15 and cultured until they reached logarithmic phase. LBD-YFP protein expression was induced by shifting from raffinose-containing medium to medium supplemented with 2% galactose, to enable activation of the GAL1 promoter. Stock solutions of steroid compounds and fungal extracts were prepared in DMSO. DMSO was added to each tube in the same volume of 10  $\mu\text{L}$  ensuring that its concentration did not exceed 1%. Uninduced, solvent, positive and negative controls were included for each binding assay. In ER- and AR-binding assays cells were exposed to steroid compounds at a final concentration of 10  $\mu\text{M}$ , while in the GR-binding assay control ligands were tested at 10 times higher concentration because the biosensor for this isoform is less sensitive.  $\text{H}_2\text{O}$  and EtOH extracts of *S. lonicerinus* were tested at final concentration of 3  $\mu\text{g}/\text{mL}$  in ER $\alpha$ / $\beta$ - and AR-LBD expressing cells, while GR expressing cells were treated with extracts at final concentration of 30  $\mu\text{g}/\text{mL}$ . Treated cells were incubated at 22°C for 14–16 h in the dark. Fluorescence was measured in 96-well format in the Fluoroskan Ascent FL fluorimeter using excitation at 485 nm and measuring emission at 538 nm. All measurements were performed in triplicate. Relative binding affinity was expressed as the fold fluorescence change between ligand-treated and ligand-free recombinant yeast cells exposed to DMSO solvent only (or oestradiol-treated cells in the case of GR-assay), normalised to 1. The binding data were analysed in Origin (OriginLab, Northampton, MA), version 9.0. Error bars correspond to the propagated standard errors of the mean.

### Heterologous expression, purification and enzyme assay of AKR1C3 and AKR1C4

For protein expression in *E. coli*, the strain BL21 (DE3) was purchased from Novagen (Merck, Germany). Plasmid constructs pET28b(+)-AKR1C3 and pET28b(+)-AKR1C4 were obtained from Dr. Chris Bunce (University of Birmingham)<sup>73</sup>. Expression, purification, and *in vitro* enzyme activity assays of recombinant AKR1C3 and AKR1C4 were performed as described in our previous work<sup>69,74,75</sup>. The pET28b(+) vectors carrying a gene encoding 6  $\times$  His-tagged human AKR1C3 or AKR1C4 under the control of a T7 promoter were used to transform chemically competent BL21(DE3) *E. coli* cells via a heat shock procedure. Transformed cells were then grown overnight in LB medium supplemented with 50  $\mu\text{g}/\text{mL}$  kanamycin in Biosan orbital shaker-incubator ES-20/60 at 37°C. Protein expression was induced by adding 0.5 mM isopropyl 1-thio-D-galactopyranoside (IPTG) and

cultures were incubated for an additional 20 h at 23°C. Cells were harvested, resuspended in 20 mM Tris–HCl pH 8.0, 5 mM imidazole and lysed by a combination of lysozyme treatment and sonication (Soniprep 150, MSE, Crawley, West Sussex, England). Lysate was centrifuged (12000×g, 4°C, 45 min) and the supernatant was loaded onto a HisTrap HP column previously equilibrated with the buffer solution (20 mM Tris–HCl pH 8.0, 0.5 M NaCl). After removal of the flow through fraction, the affinity resin was washed with five column volumes of binding buffer with 20 mM imidazole and 6 × His His-tagged protein was eluted with 5 ml of elution buffer containing 400 mM imidazole. As a final step, residual imidazole was removed from the eluted protein by size-exclusion chromatography using a Bio-Gel P-10 column (Bio-Rad, Hercules, CA, exclusion limit 20 000 daltons) equilibrated in 20 mM Tris–HCl pH 8.0, 0.1 M NaCl. The elution profile was monitored by Bradford assay<sup>76</sup>. Protein-containing fractions were pooled and frozen in small aliquots in 20 mM Tris–HCl pH 8.0, 0.1 M NaCl, 10% glycerol and 1 mM DTT at –80°C for future use in enzyme assays. Following our previously published protocols for testing the AKR1C inhibitory effects of steroid derivatives<sup>69,75,77</sup>, the potential of H<sub>2</sub>O and EtOH extracts of *S. lonicerinus* to inhibit AKR1C3 and AKR1C4 was examined. AKR1C activity was assayed by fluorimetric measurement of NADPH consumption using a Fluoroskan Ascent FL fluorimeter. Enzyme (80 µg/mL AKR1C3 or 160 µg/mL AKR1C4) was incubated with NADPH (250 µM) and 9,10 PQ (4 µM in AKR1C3 assay and 17 µM in AKR1C4 assay) in potassium phosphate buffer (100 mM, pH 6.0) and reaction progress was monitored by fluorescence spectroscopy with excitation/emission wavelengths set to 340/460 nm at 37°C every 30 s for 10 min. The catalytic activity of AKR1C was also tested in the presence of 33 µM ibuprofen (IBU) as a known inhibitor. Fungal extracts were screened for inhibition potential at a final concentration of 3 µg/mL. Blank was conducted in the absence of enzymes, while in the reaction control (Reaction) no inhibitor was added and the slope of the curve from fluorescence vs. time plots was defined as 100% enzymatic activity. All measurements were performed in triplicate. The inhibition potential of tested fungal extracts was analysed in Origin (OriginLab), version 9.0.

#### *In silico* molecular docking study of secondary metabolites from *S. lonicerinus*

Seventeen phenolic compounds that were detected in EtOH extracts of *S. lonicerinus* were chosen for further analysis by molecular docking against human AKR1C3. The three-dimensional coordinates of each compound were obtained from PubChem<sup>78</sup> and verified in the program AVOGADRO<sup>79</sup>. The geometries of three-dimensional models of these compounds were energy minimised in AVOGADRO using the conjugate gradients algorithm in an MMF94 force field with a convergence setting of 10e<sup>–7</sup>. Gasteiger partial charges were calculated for ligand atoms and ligand coordinate files were converted to PDBQT format for molecular docking using the script, “ligand.c”, in the program VEGA ZZ version 3.2.1.33. For molecular docking, the “receptor” used was an X-ray structure of AKR1C3 in complex with ibuprofen, a non-steroidal inhibitor (PDB 3R8G)<sup>80</sup>. Using the script ‘receptor.c’ in VEGA ZZ, hydrogen atoms were added to the receptor, Gasteiger partial charges were calculated and ligand coordinate files were converted to PDBQT format<sup>81</sup>. Molecular docking simulations were conducted for each of the 17 compounds in Autodock Vina using the program PyRx<sup>82,83</sup>. Docking simulations were centred on the AKR1C3 active site (x=1.80, y=30.34, z=30.25) with a search space of 25×25×25 Å and an exhaustiveness setting of 16. As a positive control, ibuprofen, the ligand present in the X-ray structure of

AKR1C3 (PDB 3R8G) was redocked into the active site with an R.M.SD of ≤ 0.6 Å using the same parameters. The resulting predicted binding energy for ibuprofen (–8.4 kcal/mol) was considered to be a threshold energy to identify compounds that could be potential AKR1C3 inhibitors. Compounds with binding energies ≥ –8.4 kcal/mol were then further analysed in the program PyMol. Docking results were analysed by superposition onto the experimental X-ray structure of AKR1C3 in complex with ibuprofen. 3D images of docking results were created in PyMol<sup>84</sup>.

#### Statistical analysis

Data with a normal distribution were analysed using univariate (ANOVA) and multivariate (MANOVA) methods, with Tukey's HSD test to determine significant differences ( $p < 0.05$ ). Pearson's correlation was applied for correlation analysis. Statistical analyses were performed using IBM SPSS version 22.0 (IBM SPSS Statistics, Armonk, NY) and Statistica version 12.01 (Tulsa, OK), while a heat map was created in Microsoft Excel (2016). Principal component analysis (PCA) was conducted using Past 4 Project software version 1.0.0.0.

## Results and discussion

#### Phylogenetic analyses

The combined ITS+LSU + *TEF1* dataset of *S. lonicerinus* and related species included 14 specimens representing 12 taxa. The dataset had an aligned length of 1823 characters, of which 1478 characters are constant, 156 are variable and parsimony-uninformative, and 189 are parsimony-informative. Maximum parsimony analysis yielded two equally parsimonious trees (TL = 492, CI = 0.811, RI = 0.739, RC = 0.599, HI = 0.189). The best model for the combined ITS + LSU + *TEF1* sequences dataset estimated and applied in the Bayesian analysis was: GTR + I + G, Iset nst = 6, rates=invgamma; prset statefreqpr=dirichlet (1,1,1,1). Bayesian analysis resulted in the same topology with an average standard deviation of split frequencies = 0.003781. Two sampled isolates of the species, *S. lonicerinus* formed a well-supported lineage (100% MP and 1 BPPs) (Figure 1). The morphology of the specimens collected in Uzbekistan, Central Asia was generally uniform with descriptions of the type specimen<sup>24,85</sup>. Also, the phylogenetic relationship of *Sanghuangporus* was the same as that previously reported<sup>8,12</sup> and our specimen matched the type sequence of *S. lonicerinus* (Figure 1). Therefore, both morphology and phylogeny support identification of the specimen as *S. lonicerinus*.

#### Mycochemical characterisation

The mycochemical analysis of EtOH, H<sub>2</sub>O, and CHCl<sub>3</sub> extracts from *S. lonicerinus* entailed quantifying quinic acid and 44 selected phenolic compounds using LC-MS/MS. Furthermore, spectrophotometric techniques were utilised to assess the phenolic profile by quantifying total phenolics content (TP) and total flavonoid content (TF). Additionally, TPR and total carbohydrate content (TC) were quantified using the same approach.

#### LC-MS/MS quantification of selected phenolic compounds

Based on LC-MS/MS quantitative analysis, only 26 compounds were detected among the 45 targeted compounds, with the most abundance in the EtOH extract (Table 1).

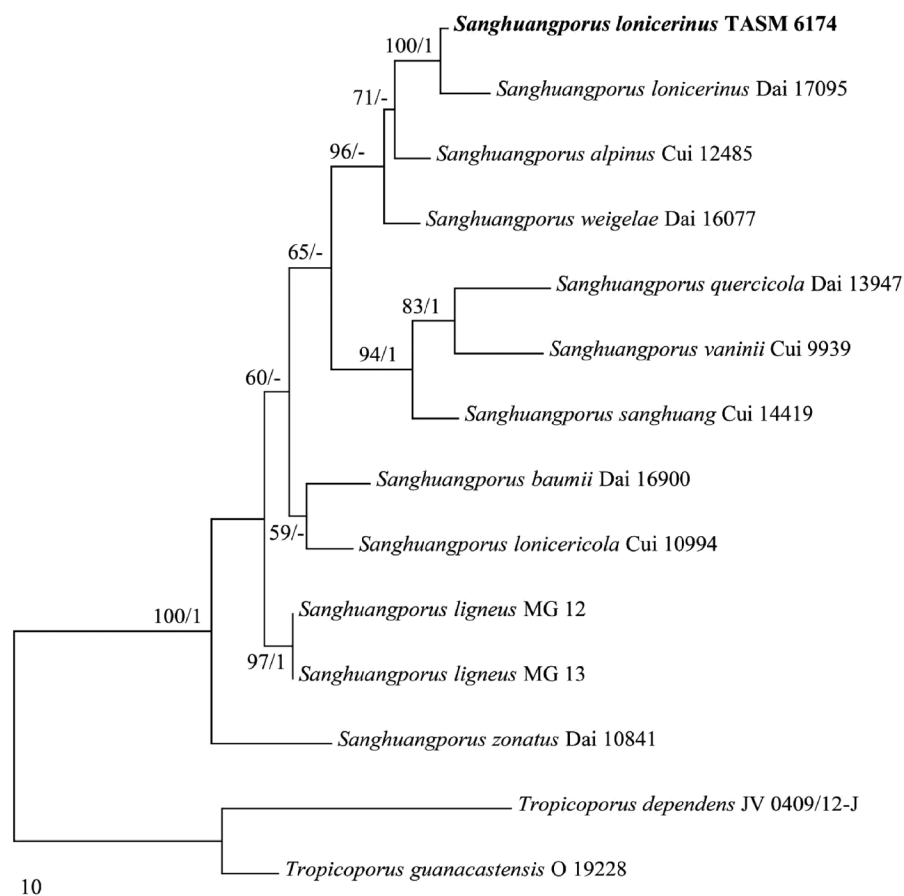


**Figure 1.** Phylogeny of *Sanghuangporus* and related species generated by maximum parsimony analysis based on combined ITS+nLSU + *TEF1* sequences. Branches are labelled with parsimony bootstrap values  $\geq 50\%$  and Bayesian posterior probabilities  $\geq 0.95$ .

These compounds were classified into different groups, including 13 flavonoids, 11 phenolic acids, quinic acid and esculetin, a coumarin derivative. Among the identified compounds, only two flavonoids, baicalein and amentoflavone, were detected in all three extracts, but both higher than the limit of detection (LoD) and beneath the limit of quantification (LoQ), while the most abundant flavonoid was quercetin-3-O-Glc+Gal ( $761.73 \pm 45.70$  ng/g d.w.), followed by luteolin ( $414.92 \pm 20.75$  ng/g d.w.) and kaempferol-3-O-glucoside ( $391.18 \pm 15.65$  ng/g d.w.) detected in EtOH extract. Conversely, apiin and rutin were only quantified in  $\text{CHCl}_3$  extract ( $77.06 \pm 3.85$  and  $112.99 \pm 3.39$  ng/g d.w., respectively). Various phenolic acids were also identified in the extracts of *S. lonicerinus*, including caffeic acid, protocatechuic acid, cinnamic acid and quinic acid among others. These compounds were found to be present in relatively higher concentrations in the EtOH extract compared to the other two analysed extracts. Notably, the EtOH extract exhibited higher levels of all detected phenolic compounds compared to the  $\text{H}_2\text{O}$  and  $\text{CHCl}_3$  extracts. Overall, the LC-MS/MS analysis demonstrated distinct phenolic profiles for each extract of *S. lonicerinus*, suggesting that the choice of solvent for extraction significantly influences the phenolic composition of these extracts.

Importantly, the results obtained in this study represent a groundbreaking account of LC-MS/MS quantification for this fungal species. This is particularly significant, as there is no existing literature data on the phenolic profile of *S. lonicerinus* or its synonyms (*Fomes lonicerinus*, *Cryptoderma lonicerinum*, *Phellinus lonicerinus*, *Porodaedalea lonicerina*, *Inonotus lonicerus*).

#### Determination of total contents: phenolics (TP), flavonoids (TF), proteins (TPR), and carbohydrates (TC)

The results revealed that the analysed *S. lonicerinus* extracts were rich in phenolic compounds among others (Table 2).

The EtOH extract exhibited the highest TP and TF ( $143.15 \pm 6.70$  mg GAE/g d.w. and  $149.24 \pm 2.74$  mg QE/g d.w., respectively), followed by the  $\text{H}_2\text{O}$  extract ( $63.18 \pm 0.71$  mg GAE/g d.w. and  $5.66 \pm 0.45$  mg QE/g d.w., respectively). The same trend was observed in TPR, quantified using the Lowry assay as well as for TC, quantified by the phenol-sulphuric assay (Table 2). These differences suggest that the choice of solvent for extraction plays a crucial role in extracting specific biochemical constituents from the fungal extracts, as mentioned above. Obtained results are in accordance with previous studies of *Sanghuangporus* spp.<sup>32,86–88</sup>, but no comparison with *S. lonicerinus* in the form of crude extracts is possible, since there is lack of literature data. Furthermore, this is the first report of TC and TPR for this fungal species.

#### Biological activities of *S. lonicerinus*

##### Antioxidant activity

The antioxidant activity of the EtOH,  $\text{H}_2\text{O}$ , and  $\text{CHCl}_3$  extracts of *S. lonicerinus* was evaluated using four different assays: DPPH radical scavenging assay, FRAP assay, NO scavenging assay, and ABTS radical scavenging assay. Among the extracts, the EtOH extract exhibited the highest DPPH and ABTS radical scavenging activity ( $34.18 \pm 1.04$  mg TE/g d.w. and  $128.89 \pm 1.01$  mg TE/g d.w.,

**Table 1.** Concentrations of selected phenolic compounds and quinic acid (ng/g d.w.).

Class	Standard compounds	Extract type (content ng/g d.w.)		
		EtOH	H <sub>2</sub> O	CHCl <sub>3</sub>
Hydroxybenzoic acids	Gallic acid	418.77 ± 37.69	294.74 ± 26.53	221.14 ± 19.90
	<i>p</i> -Hydroxybenzoic acid	3266.04 ± 195.96	1239.34 ± 74.36	120.50 ± 7.23
	Protocatechuic acid	58480.07 ± 4678.41	18634.78 ± 1490.78	3291.68 ± 263.33
	Syringic acid	6407.39 ± 1281.48	3535.40 ± 707.08	<960.00 <sup>a</sup>
Hydroxycinnamic acids	Vanillic acid	8040.34 ± 2412.10	5945.77 ± 1783.73	<1960.00 <sup>a</sup>
	Caffeic acid	132947.04 ± 9306.29	5382.44 ± 376.77	5713.50 ± 399.95
	Chlorogenic acid	315.45 ± 15.77	75.58 ± 3.78	<60.00 <sup>a</sup>
	Cinnamic acid	8072.02 ± 1614.40	<960.00 <sup>a</sup>	<960.00 <sup>a</sup>
	<i>o</i> -Coumaric acid	nd	nd	nd
	<i>p</i> -Coumaric acid	5934.04 ± 534.06	568.76 ± 51.19	499.83 ± 44.99
	3,4-Dimethoxycinnamic acid	nd	nd	nd
	Ferulic acid	1095.57 ± 109.56	324.20 ± 32.42	2079.34 ± 207.93
	Gentisic acid	nd	nd	nd
	Sinapic acid	267.09 ± 26.71	nd	nd
Cyclohexanecarboxylic acid	Quinic acid	7298.28 ± 729.83	5406.27 ± 540.63	2300.50 ± 230.05
Catechin	Epigallocatechin gallate	nd	nd	nd
Coumarins	Esculetin	1565.11 ± 93.91	<240.00 <sup>a</sup>	333.93 ± 20.04
	Scopoletin	nd	nd	nd
	Umbelliferone	nd	nd	nd
Biflavonoid	Amentoflavone	<3920.00 <sup>a</sup>	<3920.00 <sup>a</sup>	<3920.00 <sup>a</sup>
Flavanols	Catechin	nd	nd	nd
	Epicatechin	nd	nd	nd
	Kaempferol	nd	nd	nd
	Luteolin	414.92 ± 20.75	nd	141.17 ± 7.06
Flavonols	Isorhamnetin	nd	nd	nd
	Kaempferol-3- <i>O</i> -glucoside	391.18 ± 15.65	nd	<60.00 <sup>a</sup>
	Luteolin-7- <i>O</i> -glucoside	nd	nd	<60.00 <sup>a</sup>
	Myricetin	nd	nd	nd
	Quercetin	nd	nd	nd
	Quercetin-3- <i>O</i> -Glc + Gal	761.73 ± 45.70	nd	<240.00 <sup>a</sup>
	Quercitrin	<60.00 <sup>a</sup>	nd	<60.00 <sup>a</sup>
	Rutin	nd	nd	112.99 ± 3.39
	Naringenin	nd	nd	nd
	Apigenin	<960.00 <sup>a</sup>	nd	nd
Flavanone	Apigenin 7- <i>O</i> -glucoside	nd	nd	<60.00 <sup>a</sup>
	Apiin	<60.00 <sup>a</sup>	nd	77.06 ± 3.85
Flavones	Baicalein	<7800.00 <sup>a</sup>	<7800.00 <sup>a</sup>	<7800.00 <sup>a</sup>
	Baicalin	nd	nd	nd
	Chrysoeriol	nd	nd	<240.00 <sup>a</sup>
	Vitexin	nd	nd	<60.00 <sup>a</sup>
Isoflavonoids	Daidzein	nd	nd	nd
	Genistein	nd	nd	nd
Lignans	Secoisolariciresinol	nd	nd	nd

<sup>a</sup>values marked with the symbol "<"—<LOQ: detected compound – peak observed, with concentration lower than the limit of quantification (LoQ) but higher than the limit of detection (LoD). Here are the abbreviations for the parameters analysed: EtOH: hydroethanolic; H<sub>2</sub>O: hot water; CHCl<sub>3</sub>: chloroform; nd: not detected, peak not observed.

**Table 2.** Antioxidant activity, contents of total phenolics (TP), total flavonoids (TF), total proteins (TPR) and total carbohydrates (TC) and hypoglycaemic activity in analysed *S. Ionicerinus* extracts.

Parameter	Analysed extract		
	EtOH	H <sub>2</sub> O	CHCl <sub>3</sub>
DPPH (mg TE/g d.w.)	34.18 ± 1.04	4.47 ± 0.18	na
ABTS (mg TE/g d.w.)	128.89 ± 1.01	116.86 ± 6.87	40.94 ± 1.17
NO (mg TE/g d.w.)	320.55 ± 23.47	345.77 ± 18.16	n.a.
FRAP (mg AAE/g d.w.)	408.10 ± 9.42	92.74 ± 2.64	57.43 ± 2.22
TP (mg GAE/g d.w.)	143.15 ± 6.70	63.18 ± 0.71	12.70 ± 0.14
TF (mg QE/g d.w.)	149.24 ± 2.74	5.66 ± 0.45	1.21 ± 0.15
TPR (mg BSAE/g d.w.)	501.75 ± 2.58	322.12 ± 1.00	21.41 ± 0.55
TC (mg GE/g d.w.)	53.61 ± 5.53	31.89 ± 1.41	n.a.
α-amylase (% inhibition)	41.21 ± 0.79	11.02 ± 0.03	41.51 ± 1.96
α-glucosidase (% inhibition)	85.29 ± 5.58	na	39.45 ± 0.61

Here are the abbreviations for the parameters analysed: EtOH: hydroethanolic; H<sub>2</sub>O: hot water; CHCl<sub>3</sub>: chloroform; DPPH: radical scavenger capacity against 2,2-diphenyl-1-picrylhydrazyl radical, DPPH•; ABTS: radical scavenger capacity against 2,2'-azino-bis(3-ethylbenzothiazoline)-6-sulfonic acid, ABTS•<sup>+</sup>; NO: radical scavenger capacity against NO radical; FRAP: ferric-reducing antioxidant power; TP: total phenolic content; TF: total flavonoid content; TPR: total protein content; TC: total carbohydrate content; n.a.: not analysed; na: non active.

respectively) and reduction potential (408.10 ± 9.42 mg AAE/g d.w.), with the exception of NO scavenging ability where H<sub>2</sub>O extract was notable (345.77 ± 18.16 mg TE/g d.w.) (Table 2). In general, CHCl<sub>3</sub> extracts showed the lowest antioxidant potential, which is in accordance with the observed mycochemical profile, since this extract had the lowest content of polyphenolic compounds.

Correlation analysis showed high positive correlation among observed mycochemical profile and antioxidant activity. In particular, primary metabolites (TPR and TC) showed the highest positive correlation with ABTS and NO scavenging ability of the analysed extracts ( $r^2 = 0.97$  and  $r^2 = 0.96$ , respectively) which is in accordance with a previous report by Kozarski et al.<sup>89</sup>, while secondary metabolites were probably more responsible for the observed high DPPH activity and reduction potential, since  $r^2$  was in the range of 0.95–1.00 (Supplementary Figure 1(A,B)).

However, a high positive correlation was observed for both primary and secondary metabolites and antioxidant activity, which could suggest possible synergistic effects, as noted in previous studies of other fungal species<sup>10,55,90–93</sup>. On the other hand, a



negative correlation was noted solely for ferulic acid, apiin, and rutin, particularly evident in ABTS and NO scavenging activities, with coefficients of determination ( $r^2$ ) ranging from  $-0.84$  to  $-1.00$ .

The observed correlation was supported by PCA analysis where PC1 accounted for the highest proportion of variance (98.99%) and was primarily associated with phenolic composition, while PC2 captured additional variability related to antioxidant activities (1.01%). The score plot revealed distinct clustering patterns among the extracts, indicating differences in their biochemical compositions, since EtOH extract formed a separate cluster with the most of quantified compounds, with the exception of protocatechuic acid and caffeic acid (Supplementary Figure 2). Furthermore, there was a degree of intersection noted between ferulic acid and the  $\text{CHCl}_3$  extract, in agreement with LC-MS/MS findings, since this particular phenolic acid exhibited the highest abundance within this extract ( $2079.34 \pm 207.93$  ng/g d.w.). Notably, correlation analysis indicated a negative association between this acid and the antioxidant profile. The same trend can be clearly seen in the loading plot where the contribution of each variable is displayed, since ferulic acid and rutin were positioned opposite, suggesting a negative correlation with antioxidant potential.

To our knowledge, the results obtained constitute the first documentation of the antioxidant profile of crude extracts derived from *S. lonicerinus*. Previous studies have primarily explored antioxidant activity in other *Sanguangporus* species, with a particular emphasis on mycelia<sup>88</sup> and submerged fermentation<sup>87</sup>.

### Hypoglycaemic effect

Diabetes also referred to as diabetes mellitus, remains one of the most widespread epidemic illnesses globally. Because it is believed to be preventable, type 2 diabetes garners more attention compared to type 1 diabetes<sup>94</sup>. Management of type 2 diabetes involves dietary and lifestyle changes to regulate plasma glucose levels, achieved by stimulating insulin secretion or slowing starch digestion to reduce blood sugar absorption<sup>94</sup>. Inhibition of  $\alpha$ -amylase and  $\alpha$ -glucosidase activity is crucial for regulating blood glucose levels by reducing the rate of sugar absorption<sup>94</sup>. While conventional inhibitors like acarbose, miglitol, and voglibose are effective, alternative solutions are sought to mitigate their potential side effects, including particular gastrointestinal issues<sup>94</sup>. As potential alternative sources, nature has long provided a plethora of valuable compounds associated with human health benefits<sup>95</sup>. Given that mushrooms are recognised for their abundance of secondary metabolites<sup>5</sup>, which include flavonoids, phenolic acids, carbohydrates, proteins, and fatty acids, among others, and are known to possess inhibitory effects on  $\alpha$ -amylase and  $\alpha$ -glucosidase, we sought to investigate *S. lonicerinus* extracts as potential antidiabetic agents.

The *in vitro*  $\alpha$ -glucosidase and  $\alpha$ -amylase inhibition activities of three *S. lonicerinus* extracts were assessed to gauge their potential antidiabetic properties. Importantly, these results represent the first documentation of antidiabetic activity in this fungal species. The findings revealed significant inhibition of both  $\alpha$ -glucosidase and  $\alpha$ -amylase enzymes by all three fungal extracts, except for the  $\text{H}_2\text{O}$  extract, which showed no activity against  $\alpha$ -glucosidase. EtOH extract exhibited the highest inhibition potential against both enzymes, inhibiting  $85.29 \pm 5.58\%$  of  $\alpha$ -glucosidase activity, which is comparable to the medication acarbose that was used as a standard ( $86.10 \pm 2.64\%$ ) (Table 2).

Moreover,  $\text{CHCl}_3$  and EtOH extracts demonstrated similar inhibition effects against  $\alpha$ -amylase ( $41.51 \pm 1.96$  and  $41.21 \pm 0.79\%$ , respectively). These findings suggest that the EtOH extract possesses the most potent antidiabetic activity among the three

extracts tested, potentially due to its unique chemical composition since the highest amounts of tested polyphenols were found in this extract (Table 2).

Through correlation analysis, a strong positive correlation was identified between TP and TF and inhibition of  $\alpha$ -glucosidase, whereas only TF was found to be associated with inhibition against  $\alpha$ -amylase, as indicated by a heat map (Supplementary Figure 3(A)), which is in accordance with literature data<sup>96–98</sup>.

This was confirmed with detected polyphenols, since a strong positive correlation ( $r^2$  was in range from 0.86 to 0.99) was observed among phenolic acids and flavonoids, including coumarin esculetin and inhibition of  $\alpha$ -glucosidase (Supplementary Figure 3(A,B)). For example, the highest correlation was between luteolin (flavonoid) and quercetin-3-O-Glc+Gal and inhibition of  $\alpha$ -glucosidase enzyme where  $r^2$  was 0.99. Lim et al.<sup>99</sup> outlined the structural prerequisites for three flavonoids, including quercetin and luteolin as natural antidiabetic inhibitors. They highlighted the significance of the double bond between  $\text{C}_2$  and  $\text{C}_3$  of the C-ring in quercetin and luteolin for inhibiting porcine pancreatic  $\alpha$ -amylase, while the hydroxyl group (OH) at  $\text{C}_3$  of the C-ring in quercetin was associated with inhibition of  $\alpha$ -glucosidases from rat intestines. Also, molecular docking simulations indicated that luteolin has the potential to bind within the active site of  $\alpha$ -glucosidase and engage with critical amino acid residues, while subsequent *in vivo* experiments provided additional evidence that luteolin effectively reduced the absorption of glucose and triacylglyceride in rats through the inhibition of both  $\alpha$ -glucosidase and pancreatic lipase<sup>100</sup>. Furthermore, Kumar et al.<sup>98</sup> highlighted that quercetin and acarbose emerged as the most potent inhibitors of  $\alpha$ -amylase. They proposed that the increased inhibitory efficacy of these compounds might stem from the existence of a double bond between  $\text{C}_2$  and  $\text{C}_3$  in the C rings, as revealed by various analyses including docking, as outlined in their study. Similarly, inhibition of  $\alpha$ -amylase showed the strongest correlation with two flavonoids, flavone glycoside apiin and flavone luteolin ( $r^2 = 0.98$  and  $r^2 = 0.76$ , respectively), in agreement with the findings of Lim et al.<sup>96</sup>, who noted that the chemical composition of flavonoids and the presence of a double bond between  $\text{C}_2$  and  $\text{C}_3$ , along with OH groups at  $\text{A}_5$  and  $\text{B}_3$ , play crucial roles in  $\alpha$ -amylase inhibition. Conversely, the OH groups at  $\text{B}_3$  and  $\text{C}_3$  are significant for  $\alpha$ -glucosidase inhibition, enabling specific entry of the B-ring into the catalytic active site of  $\alpha$ -glucosidase<sup>96</sup>. Also, a notable correlation with antidiabetic activity (inhibition of  $\alpha$ -amylase) was observed for certain hydroxybenzoic acids, with the most prominent correlation observed for ferulic acid (a hydroxycinnamic acid), which exhibited an  $r^2$  of 0.83 (Supplementary Figure 3(B)). On the other hand, greater concentrations of phenolic acids were required for  $\alpha$ -amylase inhibition following prior interaction with starch<sup>97</sup>. This was attributed partially to the absorption of phenolic acids by starch during gelatinisation, suggesting unique inhibition mechanisms for these compounds in the  $\alpha$ -amylase assay Aleixandre et al.<sup>97</sup>. Results of correlation analysis were confirmed by PCA analysis, where the total variance was 100% (PC1 98.99% and PC2 1.01%), since most of the detected polyphenols clustered in the same quadrant, together with the EtOH extract (Supplementary Figure 4). This implies that polyphenols contribute to the observed antidiabetic activity in the EtOH extract, whereas the significant antidiabetic activity of the  $\text{CHCl}_3$  extract likely stems from the bioactivity of other compounds, given its distinct grouping in the third quadrant. Conversely, caffeic and protocatechuic acid were grouped distinctly from compounds exhibiting antidiabetic activity, consistent with prior research indicating that phenolic acids containing multiple hydroxyl (OH) groups demonstrated reduced inhibition of



antidiabetic effects Alexandre et al.<sup>97</sup>. However, further studies are warranted to elucidate the mechanisms underlying these inhibitory effects and to explore the therapeutic potential of these fungal extracts in managing diabetes.

### *In vitro* anticancer activity of *S. lonicerinus*

Relative binding affinities of extracts of *S. lonicerinus* for the ligand binding domains of ER $\alpha$ , ER $\beta$ , AR, and GR.

In order to test the relative binding affinities of EtOH and H<sub>2</sub>O extracts of *S. lonicerinus* for the LBDs of ER $\alpha$ , ER $\beta$ , AR, and GR, we used a yeast-based fluorescent assay that was optimised for preliminary screening of library of steroid derivatives, natural phenolic compounds, and phytoestrogen-rich plant extracts, as previously described<sup>67–70</sup>. Results obtained here are used to estimate the hormonal effects of the tested fungal extracts based on their steroid receptor-binding affinity. In this assay, yeast cells expressing the LBD of a hormone receptor fused to a yellow fluorescent protein (YFP) were treated with steroid hormones or fungal extract. Ligand-binding induced hormone receptor dimerization and facilitated fluorescence resonance energy transfer (FRET) between YFP monomers, resulting in a measurable increase in fluorescence intensity. Relative binding affinity was expressed as fold fluorescence change between ligand-treated and recombinant yeast cells exposed to DMSO in AR- and ER-binding assays or estradiol in GR-binding assay, with higher values corresponding to stronger affinity. As can be seen in Figure 2, both tested extracts of *S. lonicerinus* have negligible binding affinity for AR-LBD and ER $\alpha$ -LBD. The absence of androgenic and estrogenic properties makes these extracts promising candidates for further research in the development of therapeutics targeting androgen- and estrogen-dependent cancers, as well as other diseases where cell proliferation is stimulated by hormones. Following treatment with EtOH extract of *S. lonicerinus*, recombinant yeast cells expressing GR-LBD showed fold fluorescence values lower than the threshold value of 1.2, suggesting weak interaction with this receptor isoform at the tested

concentration. Among tested extracts of *S. lonicerinus*, the EtOH extract displayed stronger binding to ER $\beta$ -LBD compared to the H<sub>2</sub>O extract. The EtOH extract of *S. lonicerinus* displayed moderate binding affinity for ER $\beta$ -LBD, with a fold fluorescence enhancement of ~1.3. This extract appears to be selective for ER $\beta$  over the ER $\alpha$  isoform. While ER $\alpha$  is a trigger for proliferation of breast cancer cells, ER $\beta$  plays a protective, inhibitory role. Although researchers predominately focus on antagonists of ER $\alpha$ , due to its role in promoting tumour growth, recent studies suggest that highly selective ER $\beta$  agonists lacking affinity for ER $\alpha$  can effectively block the proliferation of ER<sup>+</sup> breast cancer cells<sup>101</sup>, indicating the potential of this extract in the treatment of estrogen-mediated breast cancer. However, further studies are necessary to determine whether the ligands identified here exhibit agonist or antagonist properties towards ER $\beta$ . Due to side effects associated with estrogen replacement therapy, there is also a growing interest in fungal extracts as new natural sources of compounds with estrogen-like activity that could offer beneficial effects in menopause and osteoporosis and provide safer alternative treatment options<sup>30</sup>. Our results are in agreement with the findings of Wang et al.<sup>30</sup> who reported that hispolon isolated from *S. lonicerinus*, exhibited stronger binding affinity for ER $\beta$  than ER $\alpha$  in a yeast two hybrid assay. This biologically active polyphenol is also known for its significant antiproliferative activity against ER<sup>+</sup>, as well as estrogen-independent breast cancer cell lines<sup>30,35</sup>. Hispolon is a structural analogue of cinnamic acid that was identified in high concentrations in our EtOH extract (Table 2). Performing *in vitro* studies Hu et al.<sup>33</sup> confirmed the estrogenic and antiestrogenic properties of EtOH extracts of *S. lonicerinus*<sup>33</sup>, consistent with the ER $\beta$ -binding ability we detected using our fluorescent biosensor in yeast. Furthermore, investigating the chemical composition of *S. lonicerinus*, Wang et al.<sup>102</sup> identified sterols that are reported to modulate the activity of nuclear receptors, such as ER and GR<sup>103</sup>, supporting our binding assay results.

### *In vitro* inhibition of human recombinant AKR1C3 and AKR1C4 activity by *S. lonicerinus* extracts

The AKR superfamily of oxidoreductases plays a crucial role in detoxification, redox transformations of carbonyl-containing substrates, and biosynthesis and metabolism of steroid hormones. However, some members of the AKR1C subfamily are also involved in the development of certain pathological conditions, such as breast, prostate and endometrial cancer and acute myeloid leukemia<sup>104,105</sup>. In addition to their overexpression in many types of cancers, AKR1C3 also contribute to drug resistance by metabolising chemotherapeutic agents, and inhibiting this isoform has been shown to restore chemosensitivity in drug-resistant cancer cells<sup>106</sup>. On the other hand, AKR1C4 preferentially acts as a 3- $\alpha$ -hydroxysteroid dehydrogenase and plays a role in xenobiotic metabolism in the liver, and inhibition of AKR1C4-mediated activity may be undesirable<sup>106</sup>. The interest in finding selective AKR1C3 inhibitors particularly in the context of cancer therapy is growing; however, none have yet been approved for clinical use. In our previous studies<sup>69,75,77</sup> several synthesised steroid derivatives have shown significant inhibition of the AKR1C3 isoform, however, published data on the inhibition of AKRs by fungal extracts is limited. There are only available reports on the aldose reductase inhibitory effects of fungal extracts<sup>107,108</sup>. For example, hispolon has been identified as a potent inhibitor of aldose reductase, a metabolic target for the treatment of diabetes<sup>35</sup>. To our knowledge, this study is the first to investigate the inhibitory effects of extracts of *S. lonicerinus* on AKR1C3 and AKR1C4 activity. Since AKRs utilise NADPH as a cofactor, to monitor the AKR1C activity we used a method based on

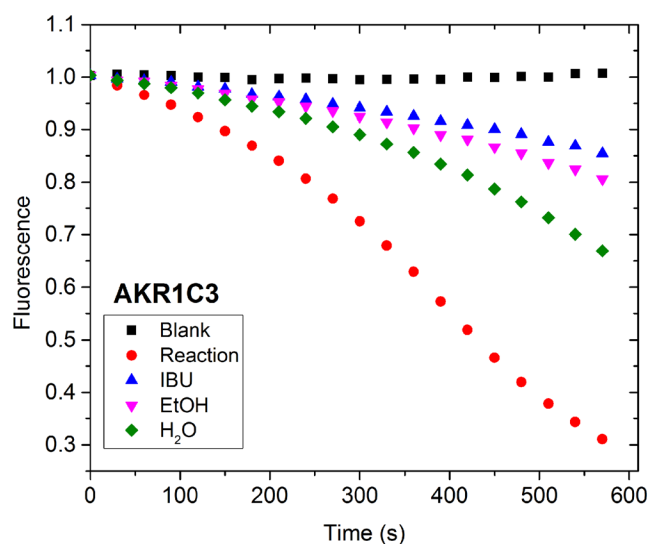


**Figure 2.** *In vitro* AKR1C3 inhibitory potential of hydroethanolic (EtOH) and hot water (H<sub>2</sub>O) extracts of *S. lonicerinus* evaluated by NADPH consumption assay. AKR1C3 activities in the presence of known inhibitor ibuprofen (IBU) or tested fungal extracts (3  $\mu$ g/mL). Blank was conducted in the absence of enzyme. AKR1C3 enzyme activity in the absence of inhibitor (Reaction) was defined as 100%. Reaction mixture components included 80  $\mu$ g/mL recombinant AKR1C3, 4  $\mu$ M PQ and 250  $\mu$ M NADPH in 100 mM potassium phosphate buffer pH 6.0. Kinetic measurements were taken at 30 s intervals during 10 min at 37  $^{\circ}$ C.

fluorimetric measurement of NADPH consumption. To evaluate the inhibition of fungal extracts, we measured their effects on the time course of reduction of 9,10-phenanthrenequinone by recombinant AKR1C3 and AKR1C4 and results are shown in Figures 3 and 4. A lower slope indicates stronger inhibition. In the absence of enzyme (Blank) there was no change in NADPH fluorescence, as expected. Based on our enzymatic assay, EtOH extract of *S. lonicerinus* has been identified as a strong AKR1C3 inhibitor, inhibiting the target enzyme by 73.9%, in the range of that identified for the known AKR1C inhibitor, ibuprofen (IBU). H<sub>2</sub>O extract of *S. lonicerinus* exhibited moderate inhibition (56.3%) against AKR1C3. Flavonoids such as 2-hydroxyflavanone, naringenin, 7-hydroxyflavone and caffeic acid phenethyl ester have been previously identified as highly potent inhibitors of the AKR1C3 isoform<sup>109,110</sup>. A possible explanation for the observed high AKR1C3 inhibition potential of the EtOH extract of *S. lonicerinus* in this study may be attributed to the presence of caffeic acid in high concentrations (Table 2), as it has been reported to inhibit this isoform<sup>110</sup>. Additionally, luteolin has also been quantified in our extract and there is data suggesting its potential to inhibit AKR1C3 as well<sup>109</sup>. On the other hand, IC<sub>50</sub> values for *p*-hydroxybenzoic acid against AKR1C3 were found to be >1000 µM<sup>110</sup>. In the presence of EtOH and H<sub>2</sub>O extracts of *S. lonicerinus*, AKR1C4 activity was weakly inhibited by 21.6% and 13.1% respectively, suggesting selectivity for the AKR1C3 isoform. Our findings indicate that extracts of *S. lonicerinus* may represent a promising source for isolating bioactive compounds to develop potential drug candidates.

#### *In silico* analysis of quantified polyphenolics against AKR1C3

As shown above, the *in vitro* AKR1C3 inhibitory potential of EtOH extracts of *S. lonicerinus* appears to be stronger than that of H<sub>2</sub>O extracts. To identify potential AKR1C3 inhibitors present among phenolic compounds detected in *S. lonicerinus* EtOH extracts, we conducted molecular docking simulations in the program Autodock Vina<sup>82</sup>. As a positive control, the known AKR1C3 inhibitor ibuprofen was redocked into the X-ray crystal structure of AKR1C3 in complex with ibuprofen (PDB 3R8G). As shown in Figure 5, Autodock Vina was able to correctly predict the binding geometry of ibuprofen from the X-ray structure with an R.M.S.D of less than 0.6 Å and a favourable binding energy of −8.4 kcal/mol. Using the same parameters, 17 phenolic compounds present in EtOH extracts of *S. lonicerinus* were docked against AKR1C3. Binding energies predicted by Autodock Vina for the top-ranking poses are listed in Supplementary Table 3.

Compounds are ranked by concentration (content ng/g d.w.) detected in EtOH extracts from *S. lonicerinus* based on Table 1. Binding energies predicted by Autodock Vina for the top-ranking pose for each compound are shown in kcal/mol, where negative values indicate energetically favourable molecular interactions. Compounds previously shown to have AKR1C3 inhibitory activity are marked with a (+), along with their reported IC<sub>50</sub> values and relevant reference in the literature if available. Compounds that are uniquely present in EtOH extracts are marked in bold. Compounds with binding energies ≥ −8.4 kcal/mol (the threshold binding energy predicted for ibuprofen), are shown in bold.

Many of the phenolic compounds detected in EtOH extracts from *S. lonicerinus* in this study were previously reported in the literature to have some level of AKR1C3 inhibitory activity

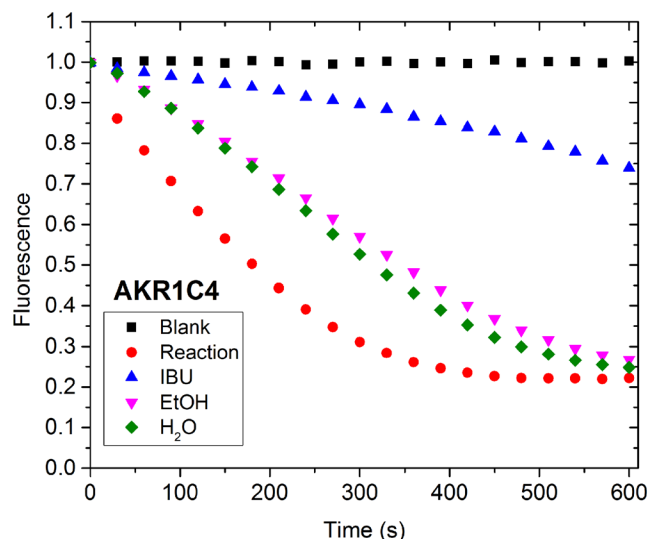


**Figure 3.** *In vitro* AKR1C4 inhibitory potential of hydroethanolic (EtOH) and hot water (H<sub>2</sub>O) extracts of *S. lonicerinus* evaluated by NADPH consumption assay. AKR1C4 activities in the presence of known inhibitor ibuprofen (IBU) or tested fungal extracts (3 µg/mL). Blank was conducted in the absence of enzyme. AKR1C4 enzyme activity in the absence of inhibitor (Reaction) was defined as 100%. Reaction mixture components included 160 µg/mL recombinant AKR1C4, 17 µM PQ and 250 µM NADPH in 100 mM potassium phosphate buffer pH 6.0. Kinetic measurements were taken at 30 s intervals during 10 min at 37 °C.

(Supplementary Table 3). As can be seen, five phenolic compounds are predicted by molecular docking to bind with similar or greater affinity than ibuprofen (≥ −8.4 kcal/mol). All of these five compounds are present in the EtOH extract and were not detected in the H<sub>2</sub>O extract. Thus, it is possible that these compounds contribute to the greater AKR1C3 inhibitory potential of EtOH extracts of *S. lonicerinus* observed experimentally. Of these, luteolin was previously reported to inhibit AKR1C3 activity with an IC<sub>50</sub> of 37 µM, similar to the micromolar IC<sub>50</sub> value reported for ibuprofen (10 µM)<sup>111,112</sup>. Molecular docking predicts that luteolin could be a competitive inhibitor that interacts with the NADP cofactor and catalytically essential amino acids Y55 and H117, in a manner similar to ibuprofen (Figure 5 panels B and C). Based on X-ray crystal structure analysis of over 60 AKR1C3-ligand complexes, AKR1C3 enzymes contain three conserved subpockets (SP1, SP2 and SP3) that are very important for ligand recognition<sup>113,114</sup>. Additional interactions are visible between luteolin and the sub-pocket known as SP1, via residues S118, N167, F306, and Y319. SP1 is involved in inhibitor binding in all known structures of AKR1C3 to date, and these molecular interactions suggest luteolin could contribute to the AKR1C3 potential of EtOH extracts of *S. lonicerinus*.

As can be seen in Supplementary Table 3, both kaempferol-3-O-glucoside (−9.1 kcal/mol) and quercetin-3-O-glucoside (−9.0 kcal/mol) are predicted by Autodock Vina to have the highest binding affinity for AKR1C3 among the tested compounds. The top-ranking binding geometries for these compounds were visualised in the program PyMol (Figure 6). Both compounds have similar chemical and three-dimensional structures, and may interact with catalytically important H117 and the NADP cofactor. Additional interactions are found with residues N167 and F306 of the AKR1C3 SP1 binding pocket, as well as Y24 and Q222 in a larger subpocket known as SP3 and W86 in the SP2 subpocket. Although further studies are

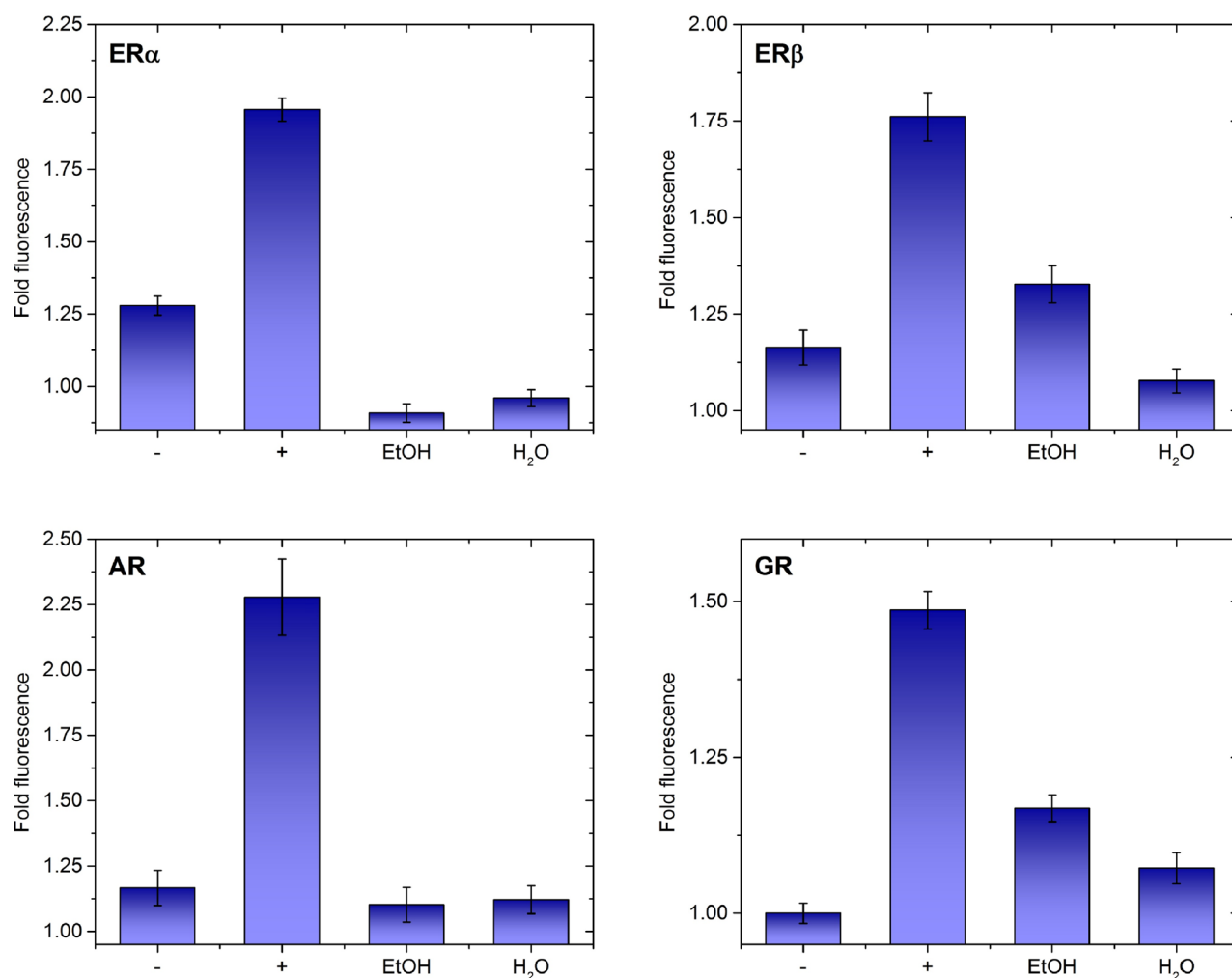


**Figure 4.** Relative binding affinities of hydroethanolic (EtOH) and hot water (H<sub>2</sub>O) extracts of *S. lonicerinus* for ligand binding domains of estrogen receptor  $\alpha$  (ER $\alpha$ ), estrogen receptor  $\beta$  (ER $\beta$ ), androgen receptor (AR) and glucocorticoid receptor (GR) measured by fluorescent screen in yeast. Relative binding affinity was expressed as fold fluorescence change between ligand-treated and recombinant yeast cells exposed to DMSO in AR- and ER-binding assays or estradiol in GR-binding assay (normalised to 1, not shown). Negative control (-) for yeast cells expressing ER $\alpha/\beta$ , AR- and GR-LBD were androstenedione, estrone and estradiol, while positive control (+) for yeast cells expressing ER $\alpha/\beta$ , AR- and GR-LBD were estrone, androstenedione and prednisolone, respectively. H<sub>2</sub>O and EtOH extracts of *S. lonicerinus* were tested at final concentration of 3  $\mu$ g/mL in all binding assays, except in the GR assay where they were added at 30  $\mu$ g/mL.

necessary, the phenolic compounds identified by molecular docking could be responsible for the AKR1C3 inhibitory potential of EtOH extracts of *S. lonicerinus*. Moreover, the fact that some of these compounds could interact with SP1, SP2 and SP3 suggests they might be candidates for design of AKR1C3 inhibitors with high specificity. Future studies could focus on structure-function analysis of purified individual phenolic compounds as AKR1C3 inhibitors.

## Conclusions

This study presents a detailed mycochemical profile of *S. lonicerinus*, highlighting its phenolic, carbohydrate, and protein content, along with the biological activities of its extracts. The EtOH extract, which is rich in quinic acid and other polyphenolic compounds, demonstrated superior antioxidant, antidiabetic, and antiproliferative properties compared to CHCl<sub>3</sub> and H<sub>2</sub>O extracts. Moreover, the EtOH extract displayed significant inhibition of  $\alpha$ -glucosidase and  $\alpha$ -amylase

activities, underscoring its potential as a natural hypoglycaemic agent. The significant inhibition of  $\alpha$ -glucosidase and  $\alpha$ -amylase, along with strong AKR1C3 inhibitory activity and moderate binding to ER $\beta$ -LBD, suggests its promise in treating estrogen-mediated cancers and other hormone-related conditions. The phenolic compounds identified in the EtOH extract of *S. lonicerinus*, particularly luteolin, kaempferol-3-O-glucoside, and quercetin-3-O-glucoside, demonstrate significant AKR1C3 inhibitory activity, suggesting their potential for the development of specific AKR1C3 inhibitors. These findings, supported by molecular docking analyses, pave the way for future research into the development of nutraceutical and pharmaceutical developments derived from *S. lonicerinus*.

This study underscores a critical need to explore under-researched fungal species like *S. lonicerinus* to fully understand their health-promoting properties, particularly in Central Asia, where this species has been studied for the first time. Our ongoing efforts aim to expand the knowledge and understanding of



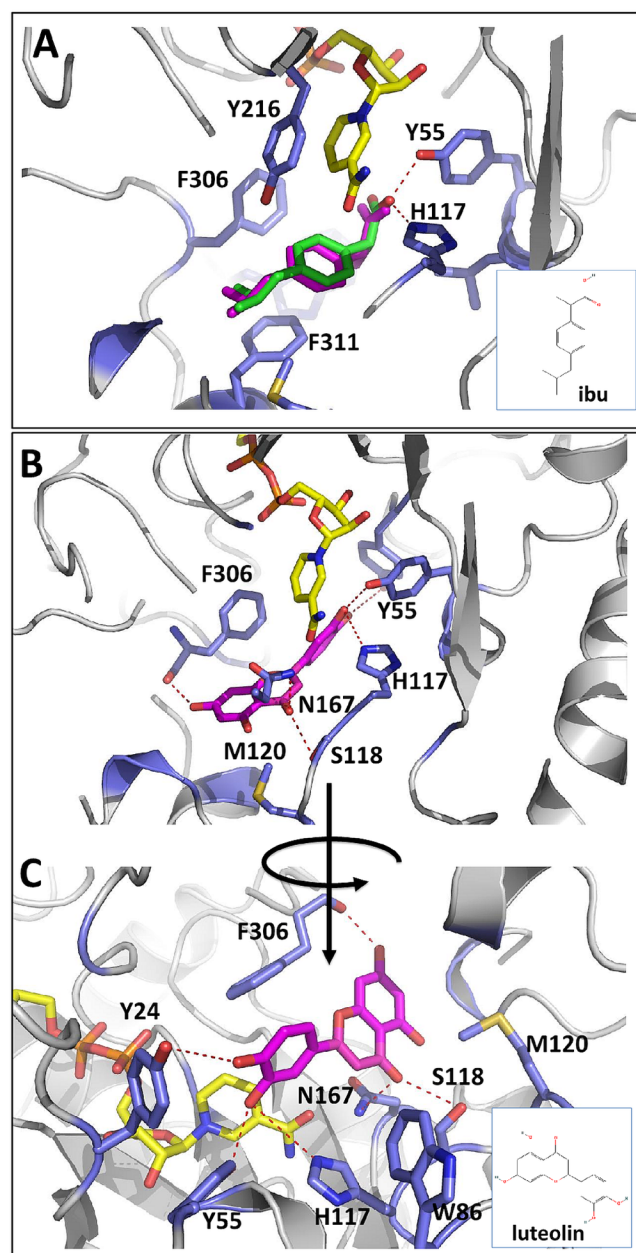


**Figure 5.** Molecular docking of luteolin against human AKR1C3. Panel A) Top ranking pose predicted by Autodock Vina during control redocking of ibuprofen (magenta sticks) against the X-ray structure of AKR1C3 in complex with ibuprofen (green sticks). Panels B and C) Top ranking pose predicted by Autodock Vina for luteolin (magenta sticks) shown in two orientations to enable visualisation of intermolecular interactions. Amino acids involved in binding are shown as blue sticks and labelled. The NADP cofactor is shown as yellow sticks.

these valuable fungi, with the goal of bringing greater awareness to their significant nutraceutical and pharmaceutical potential. By highlighting the antioxidant, hypoglycaemic, and anticancer potential of this species, our research paves the way for further investigation into both polar and non-polar bioactive compounds, with the aim of unlocking new therapeutic applications.

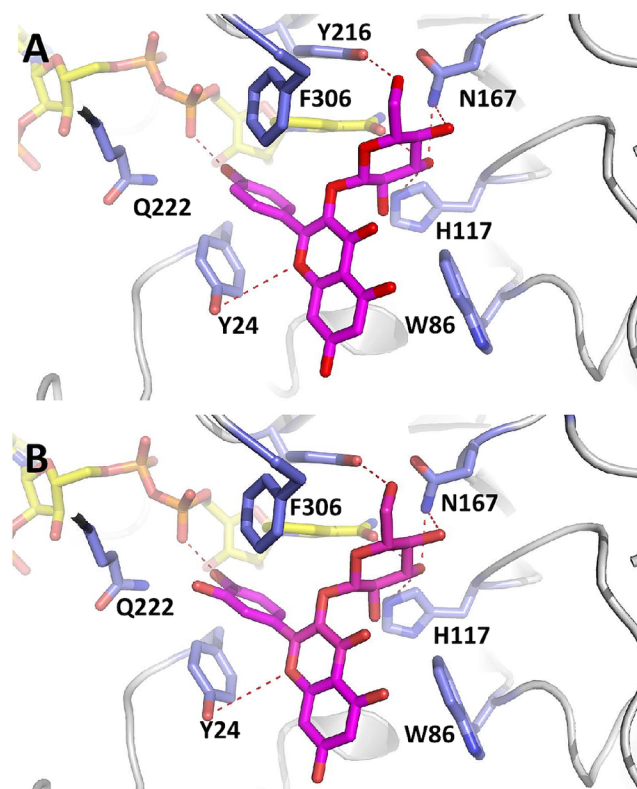


**Figure 6.** Predicted molecular interactions for the top two ranking phenolic compounds based on molecular docking. Panel A) Top ranking pose predicted by Autodock Vina for kaempferol-3-O-glucoside (magenta sticks). Panel B) Top ranking pose predicted by Autodock Vina for quercetin-3-O-Glc. Amino acids involved in binding are shown as blue sticks and labelled. NADP cofactor is shown as yellow sticks.

## Acknowledgements

The authors express their gratitude to Prof. Dr. Anđelka Čelić from the Department of Biology and Ecology, Faculty of Sciences (University of Novi Sad, Serbia), for her assistance with the anticancer aspect of this study. We also thank Prof. Dr. Marco Thines for providing access to his laboratory at the Biodiversity and Climate Research Centre, Goethe University, Frankfurt, Germany, and the German Academic Exchange Service (Grant No. 91656892) for supporting a research stay in Germany. Special thanks to Dr. Chris Bunce (The University of Birmingham) for providing the plasmid constructs pET28b(+)-AKR1C3 and pET28b(+)-AKR1C4, as well as to Dr. Blake Peterson (The University of Kansas) for the *Saccharomyces cerevisiae* FY250 strain (MATa, ura3-52, his32Δ00, leu2Δ1, trp1Δ6) and the plasmid constructs pRF4-6-hERα LBD-EYFP and pRF4-6-hERβ LBD-EYFP used in the fluorescent cellular sensor.

## Author contributions statement

YG: Conceptualisation, Data curation, Formal analysis, Funding acquisition, Investigation, Methodology, Project administration, Resources, Supervision, Validation, Visualisation, Writing –original draft, Writing – review and editing. SB: Data curation, Formal analysis, Methodology, Resources, Visualisation, Writing – original draft.



MY: Formal analysis, Methodology, Writing – review and editing. JM: Data curation, Investigation, Visualisation, Writing – original draft. NŽ: Data curation, Formal analysis, Methodology, Writing – review and editing. JJC: Formal analysis, Methodology, Writing – review and editing. EP: Data curation, Formal analysis, Methodology, Validation, Visualisation, Writing – original draft, Writing – review and editing. BA: Methodology, Data analysis. SR: Investigation, Data curation, Writing – review and editing. YWL: Investigation, Data analysis, Writing – review and editing. IA: Investigation, Data analysis, Methodology, Resources, Writing – review and editing. AMA: Data analysis, Methodology, Visualisation, Writing – original draft, Writing – review and editing. SG: Investigation, Data analysis, Writing – review and editing. WAAQIWM: Investigation, Visualisation, Writing – review and editing. MR: Conceptualisation, Data curation, Formal analysis, Funding acquisition, Investigation, Methodology, Project administration, Resources, Supervision, Validation, Visualisation, Writing – original draft, Writing – review and editing. All authors have read the final manuscript version and approved it.

## Disclosure statement

The authors declare that they have no known competing financial interests or personal relationships that might have influenced the work reported in this paper.

## Funding

This research was supported by the Agency for Innovative Development under the Ministry of Higher Education, Science, and Innovation of the Republic of Uzbekistan (Grant No. AL-8724052922-R3), the Ministry of Science, Technological Development, and Innovation of the Republic of Serbia (Grants No. 451-03-66/2024-03/200125 & 451-03-65/2024-03/200125), CAS PIFI (Grant No. 2022VBA0021), and the Science Fund of the Jiangsu Vocational College of Agriculture and Forestry (Grants No. 2024kj07 & 2023kj16).

## Data availability statement

The authors confirm that the data supporting the findings of this study are available within the article or its [supplementary materials](#).

## ORCID

Young Won Lim  <http://orcid.org/0000-0003-2864-3449>

## References

1. Rašeta MJ, Rakić MS, Čapelja EV, Karaman MA. Update on research data on the nutrient composition of mushrooms and their potentials in future human diets. In: Stojković D, Barros L, editors. Food chemistry, function and analysis, edible fungi: chemical composition, nutrition and health effects. 1st ed. London: Royal Society of Chemistry; 2022. p. 27–67.
2. Qi J, Wu J, Kang S, Gao J, Hirokazu K, Liu H, Liu C. The chemical structures, biosynthesis, and biological activities of secondary metabolites from the culinary-medicinal mushrooms of the genus *Hericium*: a review. Chin J Nat Med. 2024;22(8):676–698.
3. Wang Z, Huang K, Pu K, Li L, Jiang W, Wu J, Kawagishi H, Li M, Qi J. *Naematelia aurantialba*: a comprehensive review of its medicinal, nutritional, and cultivation aspects. Food Med Homol. 2024;2:9420072.
4. Venturella G, Ferraro V, Cirlincione F, Gargano ML. Medicinal mushrooms: bioactive compounds, use, and clinical trials. Int J Mol Sci. 2021;22(2):634.
5. Karaman M, Čapelja E, Rašeta M, Rakić M. Diversity, chemistry, and environmental contamination of wild growing medicinal mushroom species as sources of biologically active substances (antioxidants, anti-diabetics, and AChE inhibitors). In: Arya A, Rusevska K, editors. Biology, cultivation and applications of mushrooms. 1st ed. Singapore: Springer; 2022. p. 203–257.
6. Chafouz R, Karavergou S, Tsiotsoglou OS, Maskovic P, Lazari D. *Ganoderma adspersum* (*Ganodermataceae*): investigation of its secondary metabolites and the antioxidant, antimicrobial, and cytotoxic potential of its extracts. Int J Mol Sci. 2023;25(1):516.
7. Dan A, Swain R, Belonce S, Jacobs RJ. Therapeutic effects of medicinal mushrooms on gastric, breast, and colorectal cancer: a scoping review. Cureus. 2023;15(4):e37574.
8. Gafforov Y, Rašeta M, Rapior S, Yarasheva M, Wang X, Zhou L, Wan-Mohtar W, Zafar M, Lim YW, Wang M, et al. Macrofungi as medicinal resources in Uzbekistan: biodiversity, ethnomyecology, and ethnomedicinal practices. J Fungi (Basel). 2023e;9(9):922.
9. De Luca F, Roda E, Rossi P, Bottone MG. Medicinal mushrooms in metastatic breast cancer: What is their therapeutic potential as adjuvant in clinical settings? Curr Issues Mol Biol. 2024;46(7):7577–7591.
10. Rašeta M, Mišković J, Berežni S, Kostić S, Kebert M, Matavulj M, Karaman M. Antioxidant proficiency in Serbian mushrooms: a comparative study on *Hydnum repandum* L. 1753 from mycorrhizal and edible niches. Nat Prod Res. 2024;38:1–8.
11. Gafforov Y, Phookamsak R, Jiang H-B, Wanasinghe DN, Juliev M. *Ophiobolus hydei* sp. nov. (Phaeosphaeriaceae, Ascomycota) from *Cirsium* and *Phlomis* in Uzbekistan. Botany. 2019; 97(12):671–680.
12. Gafforov Y, Ordynets A, Langer E, Yarasheva M, de Mello Gugliotta A, Schigel D, Pecoraro L, Zhou Y, Cai L, Zhou LW. Species diversity with comprehensive annotations of wood-inhabiting poroid and corticioid fungi in Uzbekistan. Front Microbiol. 2020;11:598321.
13. Yatsiuk I, Saar I, Kalamees K, Sulaymonov S, Gafforov Y, O'Donnell K. Epitypification of *Morchella steppicola* (Morchellaceae, Pezizales), a morphologically, phylogenetically and biogeographically distinct member of the Esculenta Clade from central Eurasia. Phytotaxa. 2016;284(1):31–40.
14. Kan YH, Gafforov Y, Li T, Zhou LW. *Hyphodontia zhixiangii* sp. nov. (Schizoporaceae, Basidiomycota) from Uzbekistan. Phytotaxa. 2017;299(2):273–279.
15. Yuan Y, Gafforov Y, Chen YY, Wu F. A new species of *Antridium* (Basidiomycota, Polyporales) from Juniper forest of Uzbekistan. Phytotaxa. 2017;303(1):47–55.
16. Wang Z, Feng X, Liu C, Gao J, Qi J. Diverse metabolites and pharmacological effects from the Basidiomycetes *Inonotus hispidus*. Antibiotics (Basel). 2022;11(8):1097.
17. Feng X, Xie T, Wang Z, Lin C, Li Z, Huo J, Li Y, Liu C, Gao J, Qi J. Distinguishing *Sanghuangporus* from sanghuang-related fungi: a comparative and phylogenetic analysis based on mitogenomes. Appl Microbiol Biotechnol. 2024;108(1):423.

18. Gafforov Y, Rašeta M, Yarasheva M, Mykchaylova O, Tomšovský M, Lim YW, Abdullaev B, Bussmann RW, Rapior S, Sanghuangporus *Lonicerinus* Bondartsev Sheng H, et al. Hymenochaetaceae. In: Khojimatov OK, Gafforov Y, Bussmann RW, editors. Ethnobiology of Uzbekistan (ethnomedicinal knowledge of mountain communities). 1st ed. Basel, Switzerland: Springer Nature; 2023. p. 1389–1399.
19. Khojimatov OK, Gafforov Y, Bussmann RW. Ethnobiology of Uzbekistan: ethnomedicinal knowledge of mountain communities; Basel, Switzerland: Springer Nature; 2023.
20. Lu J, Su M, Zhou X, Li D, Niu X, Wang Y. Research progress of bioactive components in *Sanghuangporus* spp. *Molecules*. 2024;29(6):1195.
21. Zhong S, Sun YQ, Huo JX, Xu WY, Yang YN, Yang JB, Wu WJ, Liu YX, Wu CM, Li YG. The gut microbiota-aromatic hydrocarbon receptor (AhR) axis mediates the anticolic effect of polyphenol-rich extracts from *Sanghuangporus*. *Imeta*. 2024;3(2):e180.
22. Zhou LW, Vlasák WJ, Decock C, Assefa A, Stenlid J, Abate D, Wu SH, Dai YC. Global diversity and taxonomy of the *Inonotus linteus* complex (Hymenochaetales, Basidiomycota): *Sanghuangporus* gen. nov., *Tropicoporus excentrodendri* and *T. guanacastensis* gen. et Spp. nov., and 17 new combinations. *Fungal Divers*. 2016;77(1):335–347.
23. Zhou LW, Ghobad-Nejhad M, Tian XM, Wang YF, Wu F. Current status of 'Sanghuang' as a group of medicinal mushrooms and their perspective in industry development. *Food Rev Int*. 2022;38(4):589–607.
24. Bondartser A, Singer R. Zur systematik der polyporaceen. *Ann Mycol*. 1941;39:43–65.
25. Ryvarden L, Gilbertson RL. European polypores. 2: meripilustromyces/By Ryvarden R, Gilbertson, RL. Draw. by Gilbertson RL. and Annegi Eide. Oslo: Fungiflora; 1994. p. 394–743.
26. Shen S, Liu SL, Jiang JH, Zhou LW. Addressing widespread misidentifications of traditional medicinal mushrooms in *Sanghuangporus* (Basidiomycota) through ITS barcoding and designation of reference sequences. *IMA Fungus*. 2021;12(1):10.
27. Ghobad-Nejhad M. Collections on *Lonicera* in Northwest Iran represent an undescribed species in the *Inonotus linteus* complex (Hymenochaetales). *Mycol Progress*. 2015;14(10):90.
28. Parmasto E, Parmasto I. *Phellinus baumii* and related species of the *Ph. linteus* group (Hymenochaetaceae, Hymenomycetes). *Folia Cryptog Estonica*. 2001;38:53–61.
29. Zhang HQ, Deng GQ, Wang JZ, Hu K, Chen YL, Li TL. Study on constituents from cultures of fungus *Phellinus lonicerinus*. *Nat Prod Res Dev*. 2021;33(11):1866–1870.
30. Wang J, Hu F, Luo Y, Luo H, Huang N, Cheng F, Deng Z, Deng W, Zou K. Estrogenic and anti-estrogenic activities of hispolon from *Phellinus lonicerinus* (Bond.) Bond. et Sing. *Fitoterapia*. 2014;95:93–101.
31. Wang J, Chen B, Hu F, Zou X, Yu H, Wang J, Zhang H, He H, Huang W. Effect of hispolon from *Phellinus lonicerinus* (Agaricomycetes) on estrogen receptors, aromatase, and cyclooxygenase II in MCF-7 breast cancer cells. *Int J Med Mushrooms*. 2017;19(3):233–242.
32. Wang J, Lv H, Chen B, Huang W, Wang A, Liu L, He H, Chen J, Li S, Deng WQ. Methyl- hispolon from *Phellinus lonicerinus* (Agaricomycetes) affects estrogen signals in MCF-7 breast cancer cells and premature aging in rats. *Int J Med Mushrooms*. 2019;21(4):381–392.
33. Hu F, Wang JZ, Wu L, Huang WF, He HB, Yan XM. Estrogenic activities of alcohol extract from *Phellinus lonicerinus*. *Zhong Yao Cai*. 2016;39(3):364–340.
34. Wang JZ, Wu L, Luo YC, Zhang HQ, Huang WF, Yan XM, Zhang P. Effects of ethanol extracts of *Phellinus lonicerinus* on hepatic stellate cells of fibrosis liver in rats. *Zhong Yao Cai*. 2015;38(8):1680–1684.
35. Sarfraz A, Rasul A, Sarfraz I, Shah MA, Hussain G, Shafiq N, Masood M, Adem Ş, Sarker SD, Li X. Hispolon: a natural polyphenol and emerging cancer killer by multiple cellular signaling pathways. *Environ Res*. 2020;190:110017.
36. Iacobini C, Vitale M, Pesce C, Pugliese G, Menini S. Diabetic complications and oxidative stress: a 20-year voyage back in time and back to the future. *Antioxidants* (Basel). 2021;10(5):727.
37. Jelic MD, Mandic AD, Maricic SM, Srdjenovic BU. Oxidative stress and its role in cancer. *J Cancer Res Ther*. 2021;17(1):22–28.
38. Marinaccio L, Gentile G, Llorent-Martínez EJ, Zengin G, Masci D, Flammini F, Stefanucci A, Mollica A. Valorization of grape pomace extracts against cranberry, elderberry, rose hip berry, goji berry and raisin extracts: phytochemical profile and *in vitro* biological activity. *Food Chem*. 2025;463(Pt 2):141323.
39. Okwuosa TM, Morgans A, Rhee JW, Reding KW, Maliski S, Plana JC, Volgman AS, Moseley KF, Porter CB, Ismail-Khan R. Impact of hormonal therapies for treatment of hormone-dependent cancers (breast and prostate) on the cardiovascular system: effects and modifications: a scientific statement from the American heart association. *Circ Genom Precis Med*. 2021;14(3):e000082.
40. Mollica A, Costante R, Fiorito S, Genovese S, Stefanucci A, Mathieu V, Kiss R, Epifano F. Synthesis and anti-cancer activity of naturally occurring 2,5-diketopiperazines. *Fitoterapia*. 2014;98:91–97.
41. Blagodatski AM, Yatsunskaya M, Mikhailova V, Tiesto V, Kagansky A, Katanaev VL. Medicinal mushrooms as an attractive new source of natural compounds for future cancer therapy. *Oncotarget*. 2018;9(49):29259–29274.
42. Janjušević L, Karaman M, Šibul F, Tommonaro G, Iodice C, Jakovljević D, Pejin B. The lignicolous fungus *Trametes versicolor* (L.) Lloyd (1920): a promising natural source of antiradical and AChE inhibitory agents. *J Enzyme Inhib Med Chem*. 2017;32(1):355–362.
43. Locatelli M, Kabir A, Perrucci M, Ulusoy S, Ulusoy Hİ, Ali I. Green profile tools: current status and future perspectives. *Adv Sample Prep*. 2023;6:100068.
44. Mansour FR, Płotka-Wasyłka J, Locatelli M. Modified GAPI (MoGAPI) tool and software for the assessment of method greenness: case studies and applications. *Analytica*. 2024;5(3):451–457.
45. White TJ, Bruns TD, Lee S, Taylor J. Amplification and direct sequencing of fungal ribosomal RNA genes for phylogenetics. In: Innis MA, Gelfand DH, editors. PCR protocols: a guide to methods and applications. London: Academic Press; 1990.
46. Gardes M, Bruns TD. ITS primers with enhanced specificity for basidiomycetes-application to the identification of mycorrhizae and rusts. *Mol Ecol*. 1993;2(2):113–118.
47. Vilgalys R, Hester M. Rapid genetic identification and mapping of enzymatically amplified ribosomal DNA from several *Cryptococcus* species. *J Bacteriol*. 1990;172(8):4238–4246.
48. Rehner SA, Buckley E. A *Beauveria* phylogeny inferred from nuclear ITS and EF1- $\alpha$  sequences: evidence for cryptic diversification and links to *Cordyceps teleomorphs*. *Mycologia*. 2005;97(1):84–98.
49. Katoh K, Rozewicki J, Yamada KD. MAFFT online service: multiple sequence alignment, interactive sequence choice and visualization. *Brief Bioinform*. 2019;20(4):1160–1166.

50. Swofford DL. PAUP\*: phylogenetic analysis using parsimony (\*and other methods). version 4.0b10. Sunderland (MA): Sinauer Associates; 2002.
51. Felsenstein J. Confidence intervals on phylogenetics: an approach using bootstrap. *Evolution*. 1985;39(4):783–791.
52. Page RDM. Treeview: application to display phylogenetic trees on personal computers. *Comput Appl Biosci*. 1996;12(4):357–358.
53. Nylander JAA. MrModeltest v2. Program distributed by the author. Uppsala: Uppsala University; 2004.
54. Ronquist F, Huelsenbeck JP. MRBAYES 3: Bayesian phylogenetic inference under mixed models. *Bioinformatics*. 2003;19(12):1572–1574.
55. Karaman M, Jovin E, Malbasa R, Matavuly M, Popović M. Medicinal and edible lignicolous fungi as natural sources of antioxidative and antibacterial agents. *Phytother Res*. 2010;24(10):1473–1481.
56. Rašeta M, Popović M, Beara I, Šibul F, Zengin G, Krstić S, Karaman M. Anti-inflammatory, antioxidant and enzyme inhibition activities in correlation with mycochemical profile of selected indigenous *Ganoderma* spp. from Balkan region (Serbia). *Chem Biodivers*. 2021;18(2):e2000828.
57. Orčić D, Francišković M, Bekvalac K, Svirčev E, Beara I, Lesjak M, Mimica-Dukić N. Quantitative determination of plant phenolics in *Urtica dioica* extracts by high-performance liquid chromatography coupled with tandem mass-spectrometric detection. *Food Chem*. 2014;143:48–53.
58. Singleton VL, Orthofer R, Lamuela-Raventós RM. Analysis of total phenols and other oxidation substrates and antioxidants by means of Folin-Ciocalteu reagent. *Methods Enzymol*. 1999;99:152–178.
59. Chang CC, Yang MH, Wen HM, Chern JC. Estimation of total flavonoid content in propolis by two complementary colorimetric methods. *J Food Drug Anal*. 2002;10:178–182.
60. Lowry OH, Rosebrough NJ, Farr AL, Randall RJ. Protein measurement with the Folin phenol reagent. *J Biol Chem*. 1951;193(1):265–275.
61. Arnao MB, Cano A, Acosta M. The hydrophilic and lipophilic contribution to total antioxidant activity. *Food Chem*. 2001;73(2):239–244.
62. Espín JC, Soler-Rivas C, Wichers HJ. Characterization of the total free radical scavenger capacity of vegetable oils and oil fractions using 2,2-diphenyl-1-picrylhydrazyl radical. *J Agric Food Chem*. 2000;48(3):648–656.
63. Green CE, Wagner DA, Glogowski J, Skipper PL, Wishnok JS, Tannenbaum SR. Analysis of nitrate, nitrite and [<sup>15</sup>N]nitrate in biological fluids. *Anal Biochem*. 1982;243:709–714.
64. Benzie LFF, Strain JJ. Ferric reducing/antioxidant power assay: direct measure of total antioxidant activity of biological fluids and modified version for simultaneous measurement of total antioxidant power and ascorbic acid and concentration. *Methods Enzymol*. 1999;299:15–27.
65. Yang XW, Huang MZ, Jin YS, Sun LN, Song Y, Chen HS. Phenolics from *Bidens bipinnata* and their amylase inhibitory properties. *Fitoterapia*. 2012;83(7):1169–1175.
66. Palanisamy UD, Ling LT, Manaharan T, Appleton D. Rapid isolation of geraniin from *Nephelium lappaceum* rind waste and its anti-hyperglycemic activity. *Food Chem*. 2011;127(1):21–27.
67. Bekić SS, Marinović MA, Petri ET, Sakač MN, Nikolić AR, Kojić VV, Čelić AS. Identification of D-seco modified steroid derivatives with affinity for estrogen receptor  $\alpha$  and  $\beta$  isoforms using a non-transcriptional fluorescent cell assay in yeast. *Steroids*. 2018;130:22–30.
68. Bekić S, Petri E, Krstić S, Čelić A, Jovanović-Šanta S. Detection of isoflavones and phytoestrogen-rich plant extracts binding to estrogen receptor  $\beta$  using a yeast-based fluorescent assay. *Anal Biochem*. 2024;690:115529.
69. Šestić TL, Ajduković JJ, Bekić SS, Čelić AS, Stojanović ST, Najman SJ, Marinović MA, Petri ET, Škorić DĐ, Savić MP. Novel D-modified heterocyclic androstane derivatives as potential anticancer agents: synthesis, characterization, *in vitro* and *in silico* studies. *J Steroid Biochem Mol Biol*. 2023;233:106362.
70. Vasiljević BR, Petri ET, Bekić SS, Čelić AS, Grbović LM, Pavlović KJ. Microwave-assisted green synthesis of bile acid derivatives and evaluation of glucocorticoid receptor binding. *RSC Med Chem*. 2021;12(2):278–287.
71. Muddana SS, Peterson BR. Fluorescent cellular sensors of steroid receptor ligands. *Chembiochem*. 2003;4(9):848–855.
72. Gietz RD, Woods RA. Transformation of yeast by lithium acetate/single-stranded carrier DNA/polyethylene glycol method. *Methods Enzymol*. 2002;350:87–96.
73. Davies NJ, Hayden RE, Simpson PJ, Birtwistle J, Mayer K, Ride JP, Bunce CM. AKR1C isoforms represent a novel cellular target for jasmonates alongside their mitochondrial-mediated effects. *Cancer Res*. 2009;69(11):4769–4775.
74. Drury JE, Di Costanzo L, Penning TM, Christianson DW. Inhibition of human steroid 5 $\beta$ -reductase (AKR1D1) by finasteride and structure of the enzyme-inhibitor complex. *J Biol Chem*. 2009;284(30):19786–19790.
75. Marinović MA, Bekić SS, Kugler M, Brynda J, Škerlová J, Škorić DĐ, Řezáčová P, Petri ET, Čelić AS. X-ray structure of human aldo-keto reductase 1C3 in complex with a bile acid fused tetrazole inhibitor: experimental validation, molecular docking and structural analysis. *RSC Med Chem*. 2023;14(2):341–355.
76. Bradford M. A rapid and sensitive method for the quantification of microgram quantities of protein utilizing the principle of protein-dye binding. *Anal Biochem*. 1976;72(1–2):248–254.
77. Savić MP, Ajduković JJ, Plavša JJ, Bekić SS, Čelić AS, Klisurić OR, Jakimov DS, Petri ET, Djurendić EA. Evaluation of A-ring fused pyridine D-modified androstane derivatives for antiproliferative and aldo-keto reductase 1C3 inhibitory activity. *Medchemcomm*. 2018;9(6):969–981.
78. National Library of Medicine. PubChem. <https://pubchem.ncbi.nlm.nih.gov/> (accessed 10 June 2024).
79. Hanwell MD, Curtis DE, Lonie DC, Vandermeersch T, Zurek E, Hutchison GR. Avogadro: an advanced semantic chemical editor, visualization, and analysis platform. *J Cheminform*. 2012;4(1):17.
80. Flanagan JU, Yosaatmadja Y, Teague RM, Chai MZL, Turnbull AP, Squire CJ. Crystal structures of three classes of non-steroidal anti-inflammatory drugs in complex with aldo-keto reductase 1C3. *PLoS One*. 2012;7(8):e43965.
81. Pedretti A, Mazzolari A, Gervasoni S, Fumagalli L, Vistoli G. The VEGA suite of programs: an versatile platform for cheminformatics and drug design projects. *Bioinformatics*. 2021;37(8):1174–1175.
82. Trott O, Olson AJ. AutoDock Vina: improving the speed and accuracy of docking with a new scoring function, efficient optimization, and multithreading. *J Comput Chem*. 2010;31(2):455–461.
83. Dallakyan S, Olson AJ. Small-molecule library screening by docking with PyRx. In: Hempel J, Williams C, Hong C, editors.

- Chemical biology. Methods in molecular biology. Vol. 1263. New York (NY): Humana Press; 2015.
84. DeLano WL. PyMOL: an open-source molecular graphics tool. CCP4 Newsl Protein Crystallograph. 2002;40(1):82–92.
  85. Gafforov Y, Yarasheva M, Wang XW, Rašeta M, Rakhimova Y, Kyzmetova L, Bavlankulova K, Rapior S, Chen JJ, Langer E, et al. Annotated checklist of poroid hymenochaetoid fungi in Central Asia: taxonomic diversity, ecological roles, and potential distribution patterns. J Fungi (Basel). 2025;11(1):37.
  86. Cai C, Ma J, Han C, Jin Y, Zhao G, He X. Extraction and antioxidant activity of total triterpenoids in the mycelium of a medicinal fungus, *Sanghuangporus sanghuang*. Sci Rep. 2019;9(1):7418.
  87. Zuo K, Tang K, Liang Y, Xu Y, Sheng K, Kong X, Wang J, Zhu F, Zha X, Wang Y. Purification and antioxidant and anti-inflammatory activity of extracellular polysaccharopeptide from Sanghuang mushroom, *Sanghuangporus lonicericola*. J Sci Food Agric. 2021;101(3):1009–1020.
  88. Wang H, Ma JX, Wu DM, Gao N, Si J, Cui BK. Identifying bioactive ingredients and antioxidant activities of wild *Sanghuangporus* species of medicinal fungi. J Fungi (Basel). 2023;9(2):242.
  89. Kozarski M, Klaus A, Jakovljevic D, Todorovic N, Vunduk J, Petrović P, Niksic M, Vrvic MM, van Griensven L. Antioxidants of edible mushrooms. Molecules. 2015;20(10):19489–19525.
  90. Karaman M, Tesanovic K, Gorjanovic S, Pastor FT, Simonovic M, Glumac M, Pejin B. Polarography as a technique of choice for the evaluation of total antioxidant activity: the case study of selected *Coprinus comatus* extracts and quinic acid, their antidiabetic ingredient. Nat Prod Res. 2021;35(10):1711–1716.
  91. Tešanović K, Pejin B, Šibul F, Matavulj M, Rašeta M, Janjušević L, Karaman M. A comparative overview of antioxidative properties and phenolic profiles of different fungal origins: fruiting bodies and submerged cultures of *Coprinus comatus* and *Coprinellus truncorum*. J Food Sci Technol. 2017;54(2):430–438.
  92. Mišković J, Karaman M, Rašeta M, Krsmanović N, Berežni S, Jakovljević D, Piattoni F, Zambonelli A, Gargano ML, Venturella G. Comparison of two *Schizophyllum commune* strains in production of acetylcholinesterase inhibitors and antioxidants from submerged cultivation. J Fungi (Basel). 2021;7(2):115.
  93. Rašeta M, Kebert M, Mišković J, Kostić S, Kaišarević S, Stilinović N, Vukmirović S, Karaman M. *Ganoderma pfeifferi* Bres. and *Ganoderma resinaceum* Boud. as potential therapeutic agents: a comparative study on antiproliferative and lipid-lowering properties. J Fungi (Basel). 2024;10(7):501.
  94. Papoutsis K, Zhang J, Bowyer MC, Brunton N, Gibney ER, Lyng J. Fruit, vegetables, and mushrooms for the preparation of extracts with  $\alpha$ -amylase and  $\alpha$ -glucosidase inhibition properties: a review. Food Chem. 2021;338:128119.
  95. Barba-Ostria C, Carrera-Pacheco SE, Gonzalez-Pastor R, Heredia-Moya J, Mayorga-Ramos A, Rodríguez-Pólit C, Zúñiga-Miranda J, Arias-Almeida B, Guamán LP. Evaluation of biological activity of natural compounds: current trends and methods. Molecules. 2022;27(14):4490.
  96. Lim J, Ferruzzi MG, Hamaker BR. Structural requirements of flavonoids for the selective inhibition of  $\alpha$ -amylase versus  $\alpha$ -glucosidase. Food Chem. 2022;370:130981.
  97. Aleixandre A, Gil JV, Sineiro J, Rosell CM. Understanding phenolic acids inhibition of  $\alpha$ -amylase and  $\alpha$ -glucosidase and influence of reaction conditions. Food Chem. 2022;372:131231.
  98. Kumar A, Kumar Singh V, Kayastha AM. Studies on  $\alpha$ -amylase inhibition by acarbose and quercetin using fluorescence, circular dichroism, docking, and dynamics simulations. Spectrochim Acta A Mol Biomol Spectrosc. 2024;314:124160.
  99. Lim J, Zhang X, Ferruzzi MG, Hamaker BR. Starch digested product analysis by HPAEC reveals structural specificity of flavonoids in the inhibition of mammalian  $\alpha$ -amylase and  $\alpha$ -glucosidases. Food Chem. 2019;288:413–421.
  100. Xu H, Xu Q, Yin Z, Chen J, Zhang Q. Inhibitory activity of luteolin on  $\alpha$ -glucosidase and pancreatic lipase *in vitro* and *in vivo*. Int J of Food Sci Tech. 2024;59(6):3735–3743.
  101. Datta J, Willingham N, Manouchehri JM, Schnell P, Sheth M, David JJ, Kassem M, Wilson TA, Radomska HS, Coss CC, et al. Activity of estrogen receptor  $\beta$  agonists in therapy-resistant estrogen receptor-positive breast cancer. Front Oncol. 2022;12:857590.
  102. Wang XM, Luo YC, Guo ZY, Cao D, Zhou MX, Zhao YY, Zou K, Wang YZ. Study on the chemical constituents of *Phellinus lonicerinus*. Zhong Yao Cai. 2011;34(6):891–893.
  103. Ma L, Nelson ER. Oxysterols and nuclear receptors. Mol Cell Endocrinol. 2019;484:42–51.
  104. Velić P, Davies NJ, Rocha PP, Schrewe H, Ride JP, Bunce CM. Correction: lack of functional and expression homology between human and mouse aldo-keto reductase 1C enzymes: implications for modelling human cancers. Mol Cancer. 2010;9(1).
  105. Verma K, Zang T, Penning TM, Trippier PC. Potent and highly selective aldo-keto reductase 1C3 (AKR1C3) inhibitors act as chemotherapeutic potentiators in acute myeloid leukemia and T-Cell acute lymphoblastic leukemia. J Med Chem. 2019;62(7):3590–3616.
  106. Penning TM, Jonnalagadda S, Trippier PC, Rižner TL. Aldo-keto reductases and cancer drug resistance. Pharmacol Rev. 2021;73(3):1150–1171.
  107. Fatmawati S, Kurashiki K, Takeno S, Kim YU, Shimizu K, Sato M, Imaizumi K, Takahashi K, Kamiya S, Kaneko S, et al. The inhibitory effect on aldose reductase by an extract of *Ganoderma lucidum*. Phytother Res. 2009;23(1):28–32.
  108. He P, Zhang Y, Li N. The phytochemistry and pharmacology of medicinal fungi of the genus *Phellinus*: a review. Food Funct. 2021;12(5):1856–1881.
  109. Skarydová L, Zivná L, Xiong G, Maser E, Wsól V. AKR1C3 as a potential target for the inhibitory effect of dietary flavonoids. Chem Biol Interact. 2009;178(1–3):138–144.
  110. Li C, Zhao Y, Zheng X, Zhang H, Zhang L, Chen Y, Li Q, Hu X. *In vitro* CAPE inhibitory activity towards human AKR1C3 and the molecular basis. Chem Biol Interact. 2016;253:60–65.
  111. Byrns MC, Steckelbroeck S, Penning TM. An indomethacin analogue, N-(4-chlorobenzoyl)-melatonin, is a selective inhibitor of aldo-keto reductase 1C3 (type 2 3 $\alpha$ -HSD, type 5 17 $\beta$ -HSD, and prostaglandin F synthase), a potential target for the treatment of hormone dependent and hormone independent malignancies. Biochem Pharmacol. 2008;75(2):484–493.
  112. Brozic P, Golob B, Gomboc N, Rizner TL, Gobec S. Cinnamic acids as new inhibitors of 17 $\beta$ -hydroxysteroid dehydrogenase type 5 (AKR1C3). Mol Cell Endocrinol. 2006;248(1–2):233–235.
  113. Byrns MC, Jin Y, Penning TM. Inhibitors of type 5 17 $\beta$ -hydroxysteroid dehydrogenase (AKR1C3): overview and structural insights. J Steroid Biochem Mol Biol. 2011;125(1–2):95–104.
  114. Zang T, Verma K, Chen M, Jin Y, Trippier PC, Penning TM. Screening baccharin analogs as selective inhibitors against type 5 17 $\beta$ -hydroxysteroid dehydrogenase (AKR1C3). Chem Biol Interact. 2015;234:339–348.